REPORT DOCUMENTATION PAGE

Form Approved OMB NO. 0704-0188

1. REPORT DATE (DD-MM-YYYY)	2. REPORT TYPE	3. DATES COVERED (From - To)
06-02-2013	Final Report	1-Oct-2008 - 30-Sep-2012

4. TITLE AND SUBTITLE

Global Military Operating Environments (GMOE) Phase I: Linking Natural Environments, International Security, and Military Operations.

5a. CONTRACT NUMBER

W911NF-08-1-0453

5b. GRANT NUMBER

5c. PROGRAM ELEMENT NUMBER

611102

6. AUTHORS

Eric McDonald, Todd Caldwell, Todd Mihevc, Sophie Baker, Steven Bacon, Sara Jenkins, Don Sabol, Rina Schumer

5d. PROJECT NUMBER

5e. TASK NUMBER

5f. WORK UNIT NUMBER

7. PERFORMING ORGANIZATION NAMES AND ADDRESSES

Desert Research Institute - Reno
2215 Raggio Parkway

Reno, NV 89512 -

8. PERFORMING ORGANIZATION REPORT NUMBER

9. SPONSORING/MONITORING AGENCY NAME(S) AND ADDRESS(ES)

U.S. Army Research Office
P.O. Box 12211
Research Triangle Park, NC 27709-2211

10. SPONSOR/MONITOR'S ACRONYM(S)

ARO

11. SPONSOR/MONITOR'S REPORT NUMBER(S)

55065-EV.9

12. DISTRIBUTION AVAILIBILITY STATEMENT

Approved for Public Release; Distribution Unlimited

13. SUPPLEMENTARY NOTES

The views, opinions and/or findings contained in this report are those of the author(s) and should not contrued as an official Department of the Army position, policy or decision, unless so designated by other documentation.

14. ABSTRACT

The environmental conditions and parameters used in U.S. Army testing of materiél and equipment must replicate the environmental conditions that are anticipated for the areas of deployment. In particular, extreme climatic and physical factors must be incorporated into live testing protocols to ensure the functionality and sustainability of vehicles, weapons systems, and other developing battlefield technologies.

15. SUBJECT TERMS

Environmental characterization, terrain analysis, soil hydrology, pedology, remote sensing, LiDAR, IED detection, soils

16. SECURITY CLASSIFICATION OF:			17. LIMITATION OF ABSTRACT	15. NUMBER OF PAGES	19a. NAME OF RESPONSIBLE PERSON
a. REPORT	b. ABSTRACT	c. THIS PAGE			Eric McDonald
UU	UU	UU	UU		19b. TELEPHONE NUMBER: 775-673-7302

Report Title

Global Military Operating Environments (GMOE) Phase I: Linking Natural Environments, International Security, and Military Operations.

ABSTRACT

The environmental conditions and parameters used in U.S. Army testing of materiél and equipment must replicate the environmental conditions that are anticipated for the areas of deployment. In particular, extreme climatic and physical factors must be incorporated into live testing protocols to ensure the functionality and sustainability of vehicles, weapons systems, and other developing battlefield technologies.

The overall scope of this project was to examine soil and terrain across all four major environmental systems (Desert, Cold Region, Tropic, and Temperate systems). Research activities focused on comprehensive analysis of physical and chemical soil processes with emphasis on the flux of mass and energy at the soil?atmosphere boundary over a broad range of environmental conditions. Results are especially critical to the development and testing of technologies for the identification and defeat of IEDs (Improvised Explosive Devises). Project objectives included:

1. To establish multiple Master Environmental Reference Sites (MERS) for comprehensive characterization of soil processes that represent prevalent terrain conditions critical for military operations and testing.

2. To initiate analysis of the data collected at the established MERS to evaluate the temporal dynamics of energy fluxes under both natural and disturbed conditions in varying climatic regimes.

3. To explore and develop techniques, and collect data on soil and soil surface processes, that support the development and testing of technologies for the detection and defeat of IEDs.

4. To characterize terrain conditions at primary testing and training installations to determine terrain analogs for areas of current and future strategic interest.

The ultimate long-term goal of this research was to begin collecting data that will allow the establishment of a military environments reference database that will collate soil and terrain data and related literature to increase availability of global terrain data to the testing and training community.

Enter List of papers submitted or published that acknowledge ARO support from the start of the project to the date of this printing. List the papers, including journal references, in the following categories:

(a) Papers published in peer-reviewed journals (N/A for none)

Received		Paper
01/14/2013	4.00	Caldwell, T., McDonald, E., Bacon, S., Stullenbarger, G.. The performance and sustainability of vehicle dust courses for desert military testing: Journal of Terramechanics, Journal of Terramechanics, (12 2008): 213. doi:
01/14/2013	7.00	G. N. Flerchinger, T. G. Caldwell, J. Cho, S.P. Hardegree. Simultaneous Heat and Water (SHAW) Model: Model use, calibration, and validation, Transactions of the American Society of Agriculture and Biological Engineers, (03 2012): 0. doi:
01/14/2013	6.00	Onn Crouvi, Rivka Amit, Naomi Porat, Alan Gillespie, Eric McDonald, Yehouda Enzel. Significance of primary hilltop loess in reconstructing dust chronology, accretion rates, and sources; an example from the Negev Desert, Israel, Journal of Geophysical Research, (05 2009): 1. doi:
01/14/2013	5.00	Michael Young, Eric McDonald, Jianting Zhu, Todd Caldwell. Soil heterogeneity in Mojave Desert shrublands: Biotic and abiotic processes, Water Resources Research, (09 2012): 0. doi:
09/25/2009	1.00	S. Bacon, E. McDonald, S. Baker, T. Caldwell, G. Stullenbarger. Desert terrain characterization of landforms and surface materials within vehicle test courses at U.S. Army Yuma Proving Ground, USA, Journal of Terramechanics, ( ): . doi:
TOTAL:	**5**	

Number of Papers published in peer-reviewed journals:

(b) Papers published in non-peer-reviewed journals (N/A for none)

Received		Paper
01/14/2013	2.00	Eric McDonald, Steve Bacon, Rivka Amit, Yehouda Enzel, Onn Crouvi. Total suspended particulate matter emissions at high friction velocities from desert landforms, Journal of Geophysical Research, (09 2011): 1. doi:
TOTAL:	**1**	

Number of Papers published in non peer-reviewed journals:

(c) Presentations

Number of Presentations: 0.00

Non Peer-Reviewed Conference Proceeding publications (other than abstracts):

Received Paper

TOTAL:

Number of Non Peer-Reviewed Conference Proceeding publications (other than abstracts):

Peer-Reviewed Conference Proceeding publications (other than abstracts):

Received Paper

TOTAL:

Number of Peer-Reviewed Conference Proceeding publications (other than abstracts):

(d) Manuscripts

Received Paper

TOTAL:

Number of Manuscripts:

Books

Received Paper

TOTAL:

Patents Submitted

Patents Awarded

Awards

Graduate Students

NAME	PERCENT_SUPPORTED	Discipline
Todd Caldwell	0.40	
FTE Equivalent:	**0.40**	
Total Number:	**1**	

Names of Post Doctorates

NAME	PERCENT_SUPPORTED
Okba Al-Qadhi	0.78
Fabio Iwashita	0.10
Netra Regmi	0.08
FTE Equivalent:	**0.96**
Total Number:	**3**

Names of Faculty Supported

NAME	PERCENT_SUPPORTED	National Academy Member
Jose Luis Antinao	0.04	
Sophie Baker	0.11	
Markus Berli	0.15	
Tom Bullard	0.09	
Todd Caldwell	0.40	
Brian Fitzgerald	0.08	
Heather Green	0.12	
Janis Klimowicz	0.01	
Eric McDonald	0.07	
Todd Mihevc	0.28	
Don Sabol	0.05	
Rick Susfalk	0.03	
FTE Equivalent:	**1.43**	
Total Number:	**12**	

Names of Under Graduate students supported

NAME	PERCENT_SUPPORTED
FTE Equivalent:	
Total Number:	

Student Metrics

This section only applies to graduating undergraduates supported by this agreement in this reporting period

The number of undergraduates funded by this agreement who graduated during this period:	0.00
The number of undergraduates funded by this agreement who graduated during this period with a degree in science, mathematics, engineering, or technology fields:.....	0.00
The number of undergraduates funded by your agreement who graduated during this period and will continue to pursue a graduate or Ph.D. degree in science, mathematics, engineering, or technology fields:.....	0.00
Number of graduating undergraduates who achieved a 3.5 GPA to 4.0 (4.0 max scale):	0.00
Number of graduating undergraduates funded by a DoD funded Center of Excellence grant for Education, Research and Engineering:	0.00
The number of undergraduates funded by your agreement who graduated during this period and intend to work for the Department of Defense	0.00
The number of undergraduates funded by your agreement who graduated during this period and will receive scholarships or fellowships for further studies in science, mathematics, engineering or technology fields:	0.00

Names of Personnel receiving masters degrees

NAME
Total Number:

Names of personnel receiving PHDs

NAME
Todd Caldwell
Total Number: 1

Names of other research staff

NAME	PERCENT_SUPPORTED
Chris Ardans	0.01
Marie DelGrego	0.04
FTE Equivalent:	**0.05**
Total Number:	**2**

Sub Contractors (DD882)

Inventions (DD882)

Scientific Progress

See attachment

Technology Transfer

Desert Research Institute

SCIENCE • ENVIRONMENT • SOLUTIONS

Global Military Operating Environments (GMOE) Phase I: Linking Natural Environments, International Security, and Military Operations

Final Report - Scientific progress and accomplishments

Reporting Period: October 1, 2008 to September 30, 2012

Eric McDonald, Todd Caldwell, Todd Mihevc, Sophie Baker, Steven Bacon, Sara Jenkins, Don Sabol, and Rina Schumer.

January 30th, 2013

Prepared by

Desert Research Institute,
Nevada System of Higher Education

Prepared for

U.S. Army Research Office

Global Military Operating Environments (GMOE) Phase I: Linking Natural Environments, International Security, and Military Operations

Eric McDonald, Todd Caldwell, Todd Mihevc, Sophie Baker, Steven Bacon, Heather Green, Sara Jenkins, Don Sabol, and Rina Schumer.

Final Report: Scientific progress and accomplishments

Funding No.: W911NF0810453

Reporting Period
October 1, 2008 to September 30, 2012

Prepared by:
Desert Research Institute
2215 Raggio Parkway, Reno NV 89512

Prepared for:
U.S. Army Research Office
P.O. Box 12211
Research Triangle Park, NC 27709-2211

ABSTRACT

The environmental conditions and parameters used in U.S. Army testing of materiél and equipment must replicate the environmental conditions that are anticipated for the areas of deployment. In particular, extreme climatic and physical factors must be incorporated into live testing protocols to ensure the functionality and sustainability of vehicles, weapons systems, and other developing battlefield technologies.

The overall scope of this project was to examine soil and terrain across all four major environmental systems (Desert, Cold Region, Tropic, and Temperate systems). Research activities focused on comprehensive analysis of physical and chemical soil processes with emphasis on the flux of mass and energy at the soil-atmosphere boundary over a broad range of environmental conditions. Results are especially critical to the development and testing of technologies for the identification and defeat of IEDs (Improvised Explosive Devises). Project objectives included:

1. To establish multiple Master Environmental Reference Sites (MERS) for comprehensive characterization of soil processes that represent prevalent terrain conditions critical for military operations and testing.

2. To initiate analysis of the data collected at the established MERS to evaluate the temporal dynamics of energy fluxes under both natural and disturbed conditions in varying climatic regimes.

3. To explore and develop techniques, and collect data on soil and soil surface processes, that support the development and testing of technologies for the detection and defeat of IEDs.

4. To characterize terrain conditions at primary testing and training installations to determine terrain analogs for areas of current and future strategic interest.

The ultimate long-term goal of this research was to begin collecting data that will allow the establishment of a military environments reference database that will collate soil and terrain data and related literature to increase availability of global terrain data to the testing and training community.

Table of Contents

List of Figures

List of Tables

PROJECT OVERVIEW

The U.S. Army is rapidly transforming its war fighting doctrine to meet the complex nature of global security issues facing the U.S. The Capstone Concept for Joint Operations (CCJO) describes how joint forces will be required to operate rapidly and simultaneously in a wide range of military operations and environments in 2012–2025. Emerging and potential threats may expand to include the Caribbean Rim, Africa, Central Asia, the Middle East, SW Asia, and SE Asia. Future military operations will occur across a diverse range of natural environments and will require that U.S. forces adapt to a wide range of terrain, climate, and associated hazards within these operational environments. The U.S. Army's existing frameworks and approaches to characterize the natural environment worldwide are outdated (most circa 1955–80), oversimplified, and lack integration of current scientific knowledge of critical processes that occur in global environments. Furthermore, current technology that can extensively characterize natural environments is underutilized. Science-based analysis of major global terrain environments is required to identify the environmental variables most likely to adversely impact military testing and tactical operations.

The environmental conditions and parameters used in Army testing of materiél and equipment must replicate the environmental conditions that are anticipated for areas where the U.S. Army will be deployed. In particular, extreme climatic and physical factors must be incorporated into live testing protocols to ensure the functionality and sustainability of vehicles, weapons systems, and other emerging battlefield technologies. The research encompassed by this project was developed in support of current and anticipated issues concerning military testing and training with support of the U.S. Army Yuma Proving Ground, Natural Environments Test Office (NETO). The project and ongoing data collection facilitated by it will allow the examination of soil and terrain across all four major environmental systems (desert, cold region, tropical, and temperate systems). Focused research activities during the course of the project included comprehensive analysis of physical and chemical soil processes with emphasis on the flux of mass and energy at the soil-atmosphere boundary in various environmental conditions.

Overall Goal and Objectives

This initiative explored scientifically sound methods and technologies to provide cost-effective characterization of natural environments in tropical, temperate, desert, and cold region environments in support of military operations (testing to tactical). Project objectives included:

1. To establish multiple Master Environmental Reference Sites (MERS) for comprehensive characterization of soil and near surface processes that represent prevalent terrain conditions critical for military operations and testing.

2. To initiate analysis and numerical modeling of data collected at the established MERS to evaluate the temporal dynamics of energy fluxes under both natural and disturbed conditions in varying climatic regimes.

3. To explore and develop techniques, and collect data on soil and soil surface processes, that support the development and testing of technologies for the detection and defeat of IEDs (Improvised Explosive Devises).

4. To characterize terrain conditions at primary testing and training installations to determine terrain analogs for areas of current and future strategic interest.

A major long-term goal of this research was to begin collecting data that will allow the establishment of a military environments reference database that will collate soil and terrain data and related literature to increase availability of global terrain data to the testing and training community.

Significance and U.S. Department of Defense Value

Research established during this project provides multiple benefits to other U.S. Army and Department of Defense (DoD) programs. Weapons testing and training activities in desert, cold region, tropic, and temperate environments require a substantial investment in range instrumentation, groundtruthing, and land management of military installations. Soil and terrain properties are important parameters for all aspects of training and testing; however, science-based identification and assessment of key soil and terrain variables are either lacking or out-dated.

Specifically, our characterization of key soil analogs representing global operating environments supports a scientific assessment of the Global Military Operating Environments by the Natural Environments Test Office (YPG) that is being conducted by the Army Research Office (ARO), the U.S. Army Engineer Research and Development Center, Construction Engineering Research Laboratory (ERDC-CERL), the U.S. Military Academy (USMA), and Colorado State University (CSU). The project also provides useful information supporting DTC (Developmental Test Command) and YPG program objectives for development and testing of the Range Model and Simulator (Virtual Proving Ground: Synthetic Environment Core Area), baseline terrain information, and application of remote-sensing technologies for Warfighter and Chameleon.

The research also directly supports the ARO Environmental Sciences Program in Terrestrial Sciences, especially Broad Agency Announcement emphasis on research supporting *Terrestrial Processes and Landscape Dynamics* and *Terrain Properties and Characterization*. Results from the project to date, as well as future results of the on-going data collection facilitated by the project, directly support three primary ARO research areas: (1) “understanding the behavior of the land surface and the near-surface environment, [and] understanding the natural processes operating upon and within these domains”, (2), “modeling these environments for predictive and simulation purposes”, and (3) “[increasing]

knowledge of the properties and phenomenology of the surface and near-subsurface [which] is critical to support military operations".

Technical Approach

Our research strategy has been to develop and validate scientifically sound methods and technologies to provide cost-effective characterization of natural environments in tropical, temperate, desert, and cold region environments in support of military tactical operations. Research objectives primarily focused on soil impacts on the detection and defeat of IED's and on advancing knowledge of critical soil and terrain variables that directly supports testing of military equipment. The tasks undertaken can be summarized in the following four areas:

1. ***Development and analysis of Master Environmental Reference Sites (MERS) for comprehensive characterization of soil processes***—Multiple MERS have been established to provide long-term characterization (> 10 years) and monitoring of the soil microclimate, energy and mass flux, and associated terrain conditions, providing system developers and testers with well-established reference sites that have realistic values for soil variables that can be related to nearby test sites. The MERS locations were chosen to provide the best available analogs for desert, tropic, cold region, and temperate soils that are similar to soils and terrain commonly used for testing military equipment. All information collected from each MERS is being made readily available for the RDT&E (Research Development Test & Evaluation) community and directly supports comprehensive analysis of efforts associated with testing technology for the detection and defeat of IEDs. Specific components of this task included:

   Soil monitoring: A standardized, state-of-the-science set of instruments was developed and deployed at each MERS site to monitor, in near real time, surface and subsurface soil conditions that quantify energy and mass flux. The focus is on measurements of soil thermal properties (conductivity, capacity, and heat flux), electrical properties (dielectric permittivity and electrical conductivity), water content, water matric potential, and temperature.

   Soil characterization: Comprehensive characterization of the soil physical, chemical, hydrological, and mineralogical properties was carried out at each site.

   Surface measurements: At selected sites, geophysical characterization of the surface and near-subsurface was conducted using a variety of radar, thermal, electromagnetic, and spectroscopy methods.

2. ***Analysis of physical changes to shallowly disturbed soils: Redistribution and transformation of soil matrix***—Detailed analysis of the physical processes that occur in the soil matrix following soil disturbance (i.e., emplacement of IEDs) was conducted to advance knowledge of (1) what types of soil physical changes occur as a result of and following soil disturbance, and (2) how soil physical changes impact the propagation of electromagnetic or optical signals that

may have potential use for the detection of buried explosive devises. The goal of this task was to evaluate how temperature, and hydrologic and physical processes, change during and following shallow disturbance. We focused on two general changes to the soil related to the shallow insertion of IEDs or explosives into the soils: (1) changes in the soil matrix related to the alteration of fractures, pores, and overall density following soil disturbance, and (2) changes to the surface of the soil related to excavation of the soil during burial of IEDs, including possible soil disturbance related to foot or vehicle traffic.

3. ***Detailed terrain analysis for detection of IEDs: Microtopographic mapping using LiDAR***—We have investigated the use of state-of-the-art LiDAR technology for mapping surface topography at a resolution high enough to detect features indicative of IED presence. This work has shown the great potential of such technology for counter IED efforts, while indicating that the greatest challenge involved lies in processing datasets of the magnitude required for this type of task. By assimilating existing toolsets and routines, datasets large enough to detect 2mm diameter wire stretched across a desert surface, have been rendered. Furthermore, the path has been paved for the development of the analytical methods required for rendering even higher resolution datasets – this will allow superior surface textural analysis and ultimately greater IED detection capability.

4. ***Characterization of terrain conditions at key testing and training facilities*** —We have carried out extensive terrain characterization efforts for six test courses at key military installations that represent a broad spectrum of climatic and physiographic settings, and thus provide terrain analogs for most areas of potential deployment. These data, which include geotechnical, soil, and landscape parameters, will allow the similarity and differences of the testing conditions to the areas of deployment to be assessed, as well as providing baseline datasets for test course sustainability efforts.

PROJECT ACCOMPLISHMENTS

1. Development and Analysis of Master Environmental Reference Sites (MERS) for Comprehensive Characterization of Soil Processes

1.1.1 Introduction

Ongoing monitoring of soil and climate interactions has been a primary goal of this GMOE initiative. Long-term soil monitoring has been key to advancing our understanding of subsurface soil processes, which are likely to influence effective detection of IEDs. Soil properties that might influence the effectiveness of detection methods include soil composition and chemistry, soil structure, and the spatial/temporal heterogeneity of soil variables.

During the course of the project, a total of seven soil monitoring stations (MERS) have been established in a range of locations, including a large multi-plot station at the Countermine Facility at Yuma Proving Ground (YPG), two stations at the Joint Experimental Range Complex (JERC) sites at YPG, one at the University of Nevada Reno's Agricultural Experimental Station (NAES), one at Fort AP Hill, Virginia, one at the Sage Hen experimental forest in northern California, and one in Panama. Site locations were selected based on:

1. Degree to which they represent analogs for current and potential areas of combat for the U.S. Army,
2. Site security, favoring locations where minimal disturbance was anticipated, and
3. Site accessibility, as data cards need to be collected periodically, and routine maintenance of monitoring equipment needs to be performed.

Remote and automated monitoring systems were deployed at each testing site for *in situ* measurements of soil thermal properties (conductivity, capacity, and heat flux), electrical properties (dielectric permittivity and electrical conductivity), water content, and temperature, in both natural and disturbed soils. The measurement of meteorological conditions was also implemented. The sensor array employed for soil data collection was continually evaluated and improved as lessons were learnt during MERS site development. The most recent set of sensors is shown in Table 1, though manufacturer may vary somewhat by site. The soils at each site were also characterized in detail using field observations and extensive laboratory analysis of samples taken from each soil horizon.

The setup, data collection, and preliminary results from two of the MERS sites – those at the Countermine Facility and at the JERC sites – are described in more detail below, followed by an example of how MERS technology and methods have been applied in a hydrologic modeling study.

Table 1. Soil monitoring sensor array

***In situ*, [1]continuous monitoring**	**Manufacturer**	**State Variable(s)**	**[2]Surface**	**[3]Buried**
Dual Probe Heat Pulse	30East	Volumetric heat capacity, thermal diffusivity, thermal conductivity, soil water content	x	x
Time Domain Reflectometer	Dynamax, CSI	Water content, apparent dielectric permittivity, electrical conductivity	x	x
Heat Dissipation Sensor	CSI	Average soil temperature used for ground conduction		x
Soil Heat Flux Plate	Hukseflux	Heat flux density		x
Averaging Thermocouples	CSI	Ave soil temperature used for ground conduction		x
Tensiometers	SMS, Soil Moisture	Soil matric potential in wetter soils		x

***In situ*, continuous monitoring surface based**	**Manufacturer**	**State Variable(s)**	**[2]Surface**	**[3]Buried**
	REBS	Net radiation (incoming – reflected)	x	
Solar Radiation	Eppley	Incoming solar radiation	x	
Surface temperature IR	Apogee	Continuous surface temperature	x	
Eddy covariance (open path IRGA, 3D sonic anemometer, Temp/Humidity sensors, etc.)	CSI	Heat, vapor, and CO_2 flux	x	

Surface based, [4]manual	**Manufacturer**	**State Variable(s)**	**[2]Surface**	**[3]Buried**
Ground penetrating radar	PulseEkko and Noggin	Apparent dielectric permittivity, ~water content, ~silt/clay	x	
Electromagnetic induction	Geonics	Salinity, resistivity	x	x
Neutron attenuation	Troxler	Bulk soil density, water content	x	x
Air permeameter	In house	Air/gas permeability	x	x
Hydraulic parameters	In house	Conductivity, water retention, porosity	x	x
Penetration resistance	Agridry	Soil strength	x	
Large Aperture Scintillometer	Scintec	Sensible heat flux	x	
Broadband Thermal Camera	FLIR	Surface temperature/emissivity	x	

Laboratory based	**Manufacturer**	**State Variable(s)**	**[2]Surface**	**[3]Buried**
Laser diffraction	Micromeritics	Particle size distribution		
Gas phase adsorption	Micromeritics	Specific surface area		
Tri-axial shear strength	Wille Geotechnik	Soil strength, tensile proof, modulus of elasticity, Poisson's ratio, static and dynamic testing		
Dual Probe Heat Pulse	30 East	Volumetric heat capacity, thermal diffusivity, thermal conductivity, soil water content		

[1]Continuous monitoring: automated, real-time data acquisition
[2]Surface deployed sensor
[3]Buried: sensor installed below the soil surface at depth
[4]Manual: measurement requires manual activation

1.1.2 MERS Set-up and Monitoring at the Countermine Facility, Yuma Proving Ground

Four boxes, previously constructed by YPG personnel, were excavated and reinforced by the Desert Research Institute in January 2010. The boxes were planned, in conjunction with Countermines and NETO personnel, to utilize the GMOE conceptual model of a Master Environmental References Site (MERS, Figure 1). Automated data acquisition systems were operational in 11 February 2010 in undisturbed soil adjacent to four plywood boxes.

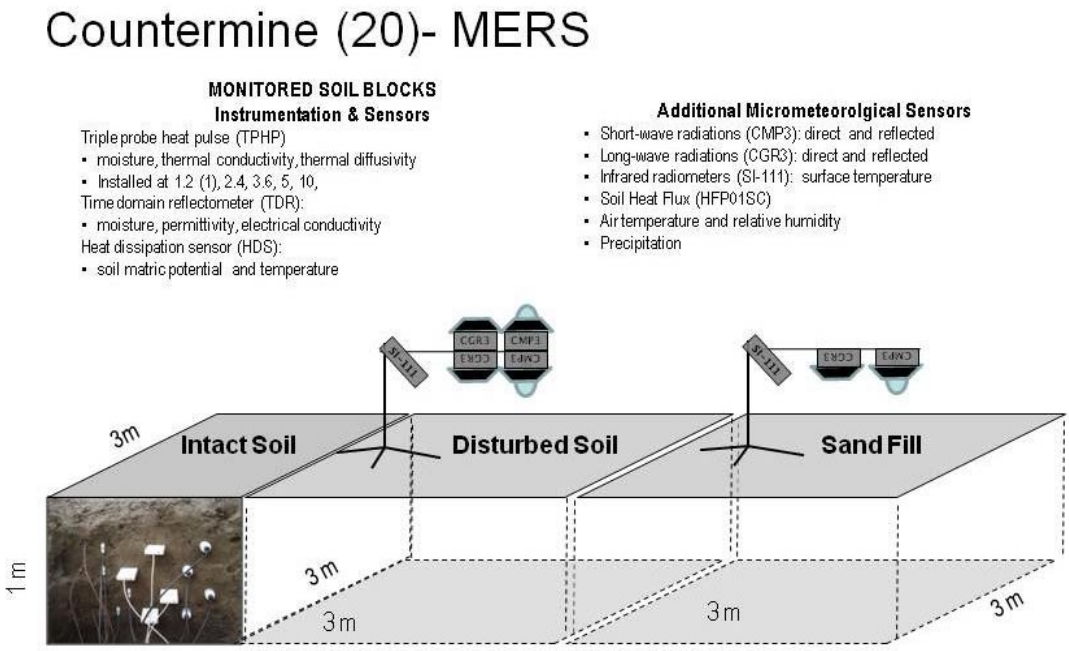

Figure 1. Conceptual design of the Countermine soil boxes.

An area 3x3m was excavated to the south of the wooden boxes. The excavated soil was homogenized and simultaneously repacked and instrumented as the 'Disturbed' plot (Figure 1). A second, adjoining, 3x3m plot was excavated and filled with construction sand to create the 'Sand' plot.

Each 3x3x1m box was subdivided into 1m^2 blocks for instrumentation (Figure 2) to measure *in situ* soil thermal (conductivity, capacity, and heat flux) and electrical properties (dielectric permittivity and electrical conductivity). Additional measurements of solar radiation (four components), air temperature and relative humidity, and precipitation are also collected and transferred in real-time (3 sec updates) to a display within the Countermine facility.

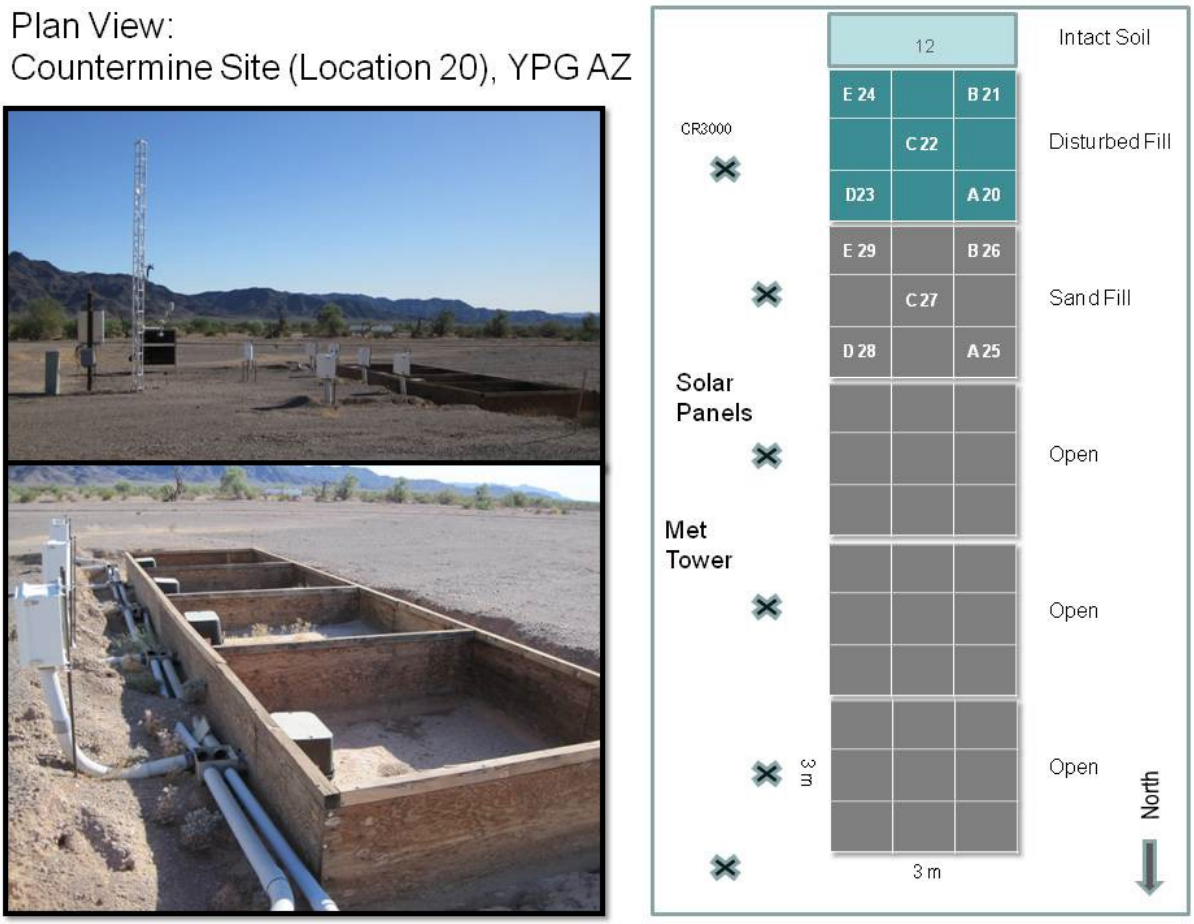

Figure 2. Photograph and plan view of the Countermine soil boxes.

Each box is set up to be independently monitored using CR3000 data loggers by Campbell Scientific, Inc. (CSI, Logan, UT) and a variety of soil moisture and atmospheric sensors (Figure 3). Soil thermal properties are monitored using tri-probe, heat-pulse (TPHP) sensors constructed by East 30 Sensors, Inc. (Pullman, WA). The TPHP consists of three 1.5 cm long needles spaced 6 mm apart. One needle contains a heating element; the others contain thermistors. Thermal properties are determined by monitoring the arrival and dissipation of a heat pulse between the needles. Soil heat flux is monitored using a heat flux plate (HFP01SC) manufactured by Hukseflux (Delft, The Netherlands). Matric potential, commonly referred to as capillary potential, is the negative pressure (when soil moisture is below saturation) of the capillary and adsorptive forces in the soil matrix. Heat Dissipation Sensors (HDS) from CSI (CS-229) are used to measure matric potential, which is computed based on heat dissipation from a controlled-source diode. Soil temperature is monitored with the same probe simply by measuring the soil temperature at the thermocouple prior to heating.

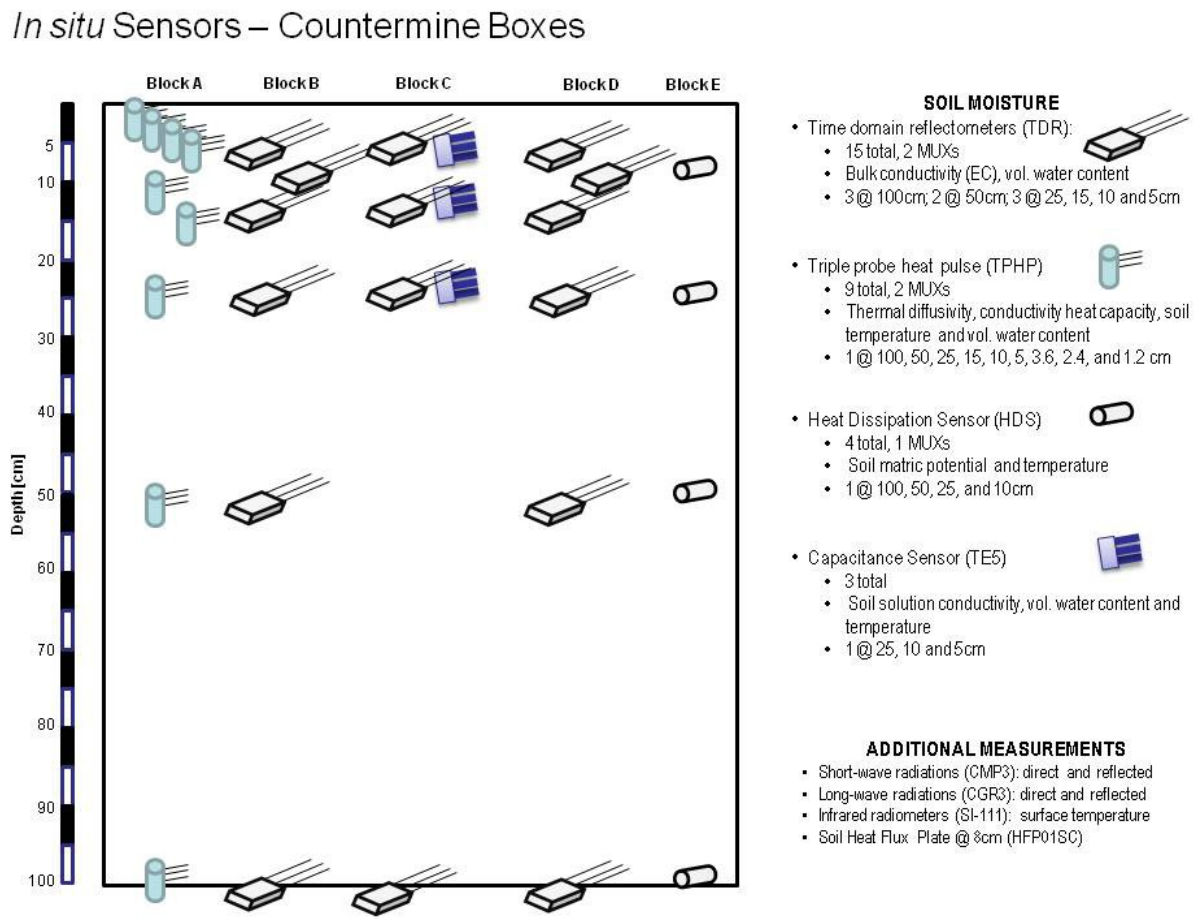

Figure 3. Profile view of the sensors installed in each soil box. Each soil box has five monitored blocks utilizing the arrangement of specified sensors.

Soil moisture is measured by multiple sensors utilizing both soil thermal (TPHP above) and dielectric properties. Dielectric sensors determine soil moisture (and electrical properties) through electromagnetic (EM) wave propagation along wave guides embedding in the soil. Two EM methods are deployed: time domain reflectometry (TDR) and capacitance (5TE). Time domain reflectometry generates a precise, high frequency EM pulse via a TDR100 (CSI) at the surface which propagates along a coaxial cable, terminating at a wave guide (or 3-rod probe, 20- cm in length). The EM reflection is recorded by the TDR100 which uses an algorithm to determine travel time and relative permittivity to then compute volumetric water content. Electrical conductivity based upon EM attenuation is also recorded. High precision oscillators are used to generate lower frequency EM pulses in the 5TE capacitance probe.

Additional meteorological sensors were installed at each box, allowing the monitoring of air temperature, relative humidity (HPM45C, Vaisala, Boulder, CO), net radiation (CRN1, CGR3, and CMP3, Kipp and Zonen, Bohemia, NY), surface temperature (by infrared radiometer) (SI-111, Apogee, Logan UT), wind speed and direction (034B Anemometer, Met One Instruments Inc., Rolette, TX), and precipitation (TE525, Texas Weather Instruments, Dallas, TX).

Additional Soil Characterization:

Three soil profiles within 10m of the boxes were excavated and sampled (18 samples in total). Furthermore, during filling and installation of boxes, soil samples were collected every 25-cm to: 1) ensure decent homogeneity of the repacked soils, 2) determine repacked bulk density, and 3) characterize the general soil properties (12 samples). All soils sampled were analyzed by the DRI Soil Characterization and Quaternary Pedology Laboratory (Table 2). For each of the three soil profiles, a representative soil sample was collected from each genetic soil horizon identified in the field. Soil samples were oven dried at 105°C for 24 hours and the gravel fraction (>2mm) removed using a No. 10 sieve. All laboratory analysis was performed on the fine earth fraction (<2mm).

Table 2. Soil lab analyses and methods.

Analysis	Method	Reference:
Particle Size Distribution	Laser light scattering	Gee and Or, 2002
Calcium Carbonate	Chittick apparatus	Dreimanis, 1962; Machette, 1986
Soil pH	pH Meter	Thomas, 1996
Electrical Conductivity	Conductivity Bridge	Rhoades, 1996
Bulk Density	Clod and Excavation	Grossmann and Reinsch, 2002

Preliminary Results – Soil Data:

Laboratory results for one of the soil profiles sampled adjacent to the four boxes is presented in Table 3. Of note, a very distinct buried soil (Btkyb) was observed at 64-cm depth around the excavated area (Figure 4). This soil is extremely red (due to iron oxides), saline, and gravelly.

Table 3. Laboratory results for one of the soil profiles adjacent to the Countermine soil boxes.

Depth			Hor.	MOIST	GRAV.	SAND	SILT	CLAY	OM	pH	SALT	xCO_3
- cm -				- g g^{-1} -	- % -	- % -	- % -	- % -	- % -		- mg g^{-1}	- % -
0	-	4	Av	0.01	32.9	38.3	41.1	20.7	1.40	7.89	0.38	1.51
4	-	9	AC	0.01	13.0	64.0	29.3	6.7	0.91	7.89	0.46	0.88
9	-	23	Ck	0.00	63.3	87.3	9.7	3.0	0.48	7.91	0.59	0.26
23	-	49	Cky1	0.00	61.8	96.0	2.5	1.4	0.41	7.93	4.41	0.21
49	-	64	Cky2	0.00	66.3	97.3	1.6	1.1	0.30	7.98	3.49	0.25
64	-	100	Btkyb	0.01	62.6	77.5	14.6	7.9	1.22	7.93	7.63	1.11

Figure 4. Soil profile sampled at Countermine Box Set (CMBS). Note buried soil at 64 cm depth.

The soil above the buried contact was approximately 30-60 cm thick. The surface was characterized by a moderately developed desert pavement over a thin (~4cm) vesicular Av horizon, composed primarily of eolian dust. The spatial distribution and heterogeneity of the contact between the surface and buried soil is currently unknown.

Monitored time-series data:

Note: The data presented herein should be used with caution. The precipitation at YPG during the month prior to the onset of monitoring was quite high resulting in wet initial soil conditions. Both moisture and soil temperature needed time (~90 days) to equilibrate to be more representative of the normal soil microclimate.

Results presented relate to the disturbed soil and the sand filled box. The disturbed, homogenized soil should be considered a mixture of the buried soil and the surface soil. The time-series of basic meteorological data is presented in Figure 5. Several precipitation events were recorded including a 20 mm event that occurred on March 7, 2010.

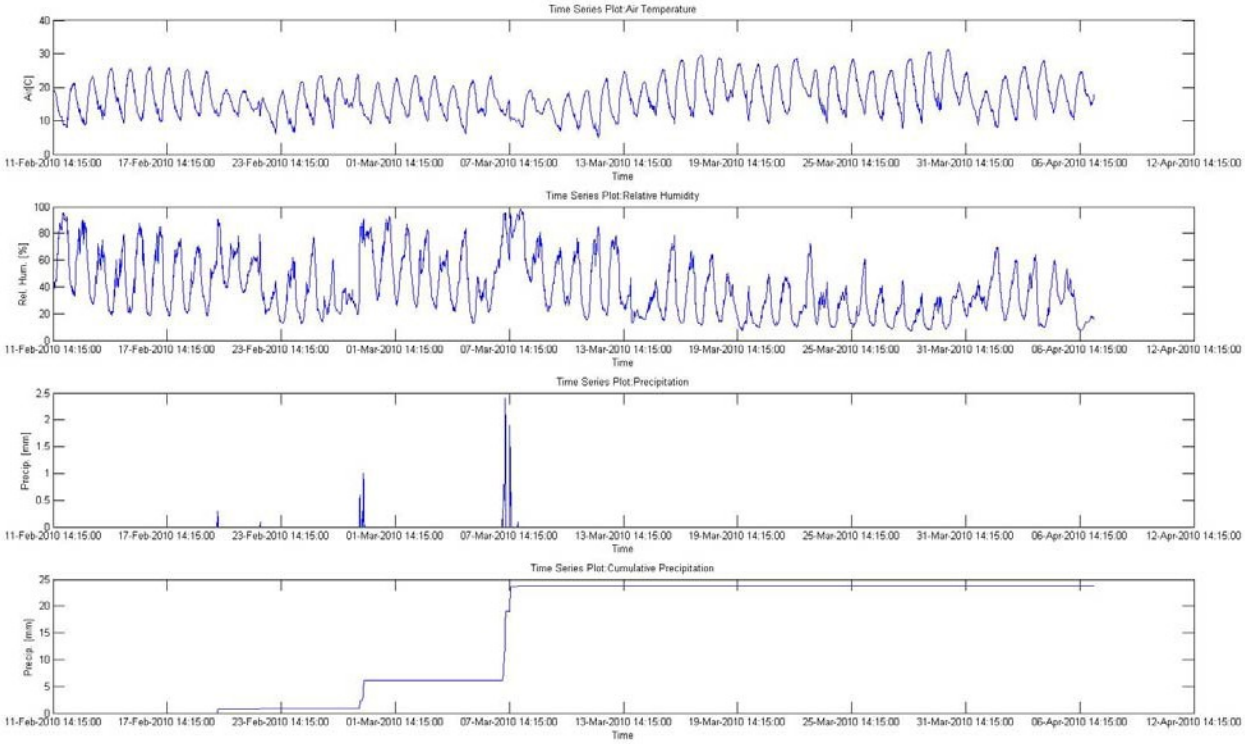

Figure 5. Basic meteorological data - air temperature, relative humidity, and precipitation (frequency and cumulative total).

Soil moisture and bulk electrical conductivity (EC) data from the TDR sensors at the disturbed plot are presented in Figures 6 (block 21) and 7 (Block 23), and for the sand box, in Figures 8 (Block 26) and 9 (Block 28). Note the diurnal effect of temperature on the EC values, and the effect of the precipitation events on soil moisture. The large event on March 7 propagated to the bottom of the box (>100-cm probe). Lastly, the two soils, disturbed and sand, have dramatically different EC values: very low for sand and very dynamic for the disturbed soil.

Moisture content, thermal properties and temperature from the triple-probe heat pulse (TPHP) sensors are presented for depths of 1.2 cm (Figure 10), 3.6 cm (Figure 11), 5 cm (Figure 12), 10 cm (Figure 13) and 15 cm (Figure 14) within the disturbed soil. Note the dependence of thermal conductivity on water content and soil temperature, particularly near the surface.

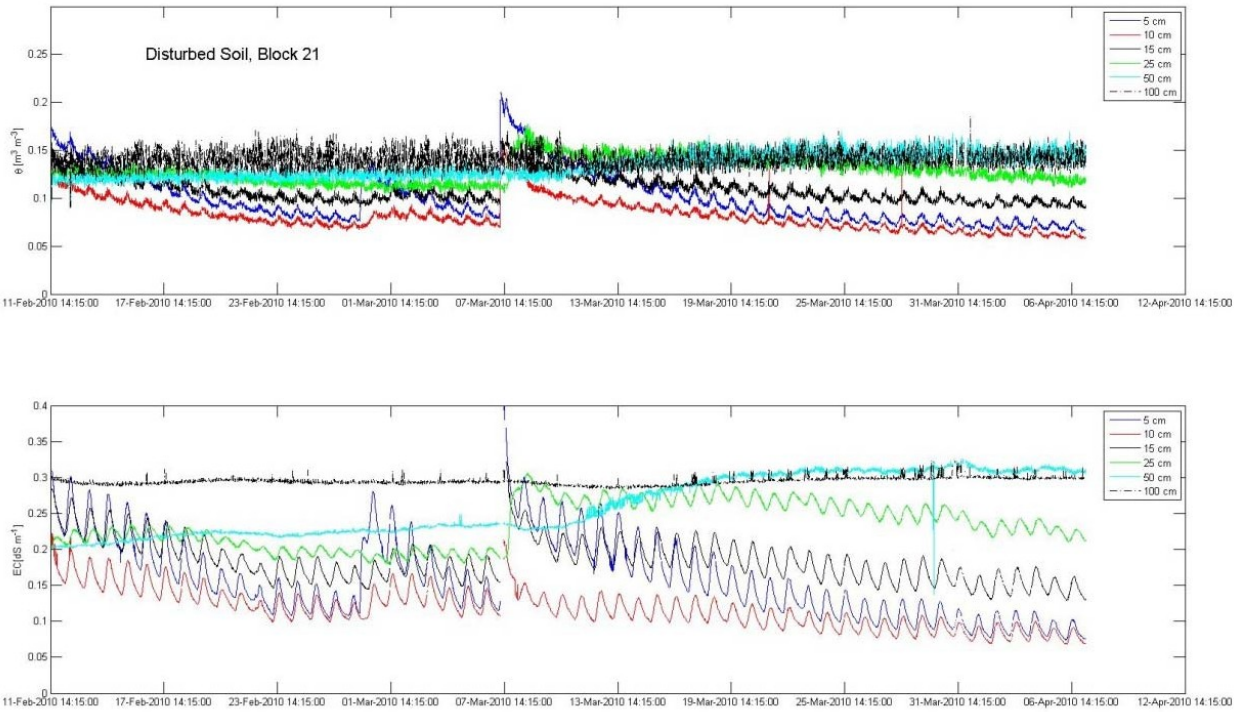

Figure 6. Time series of TDR-derived soil moisture (θ) and bulk electrical conductivity (EC) from block 21 in the disturbed soil plot.

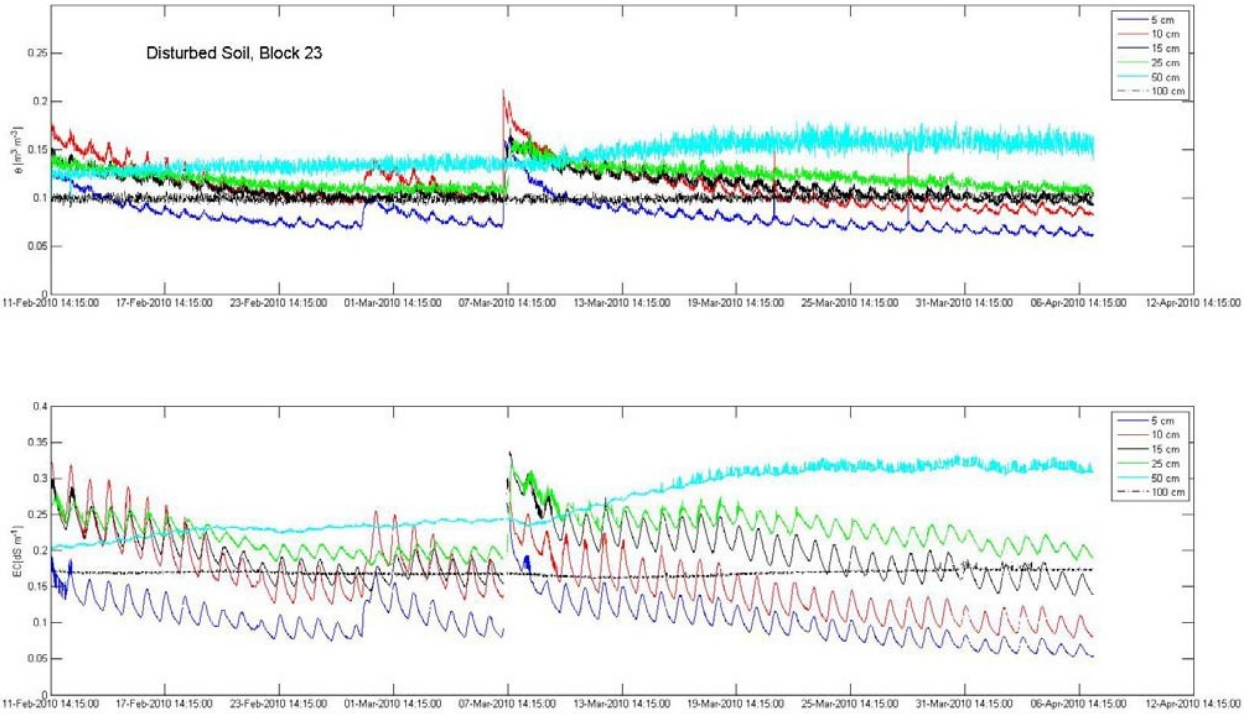

Figure 7. Time series of TDR-derived soil moisture (θ) and bulk electrical conductivity (EC) from block 23 in the disturbed soil plot.

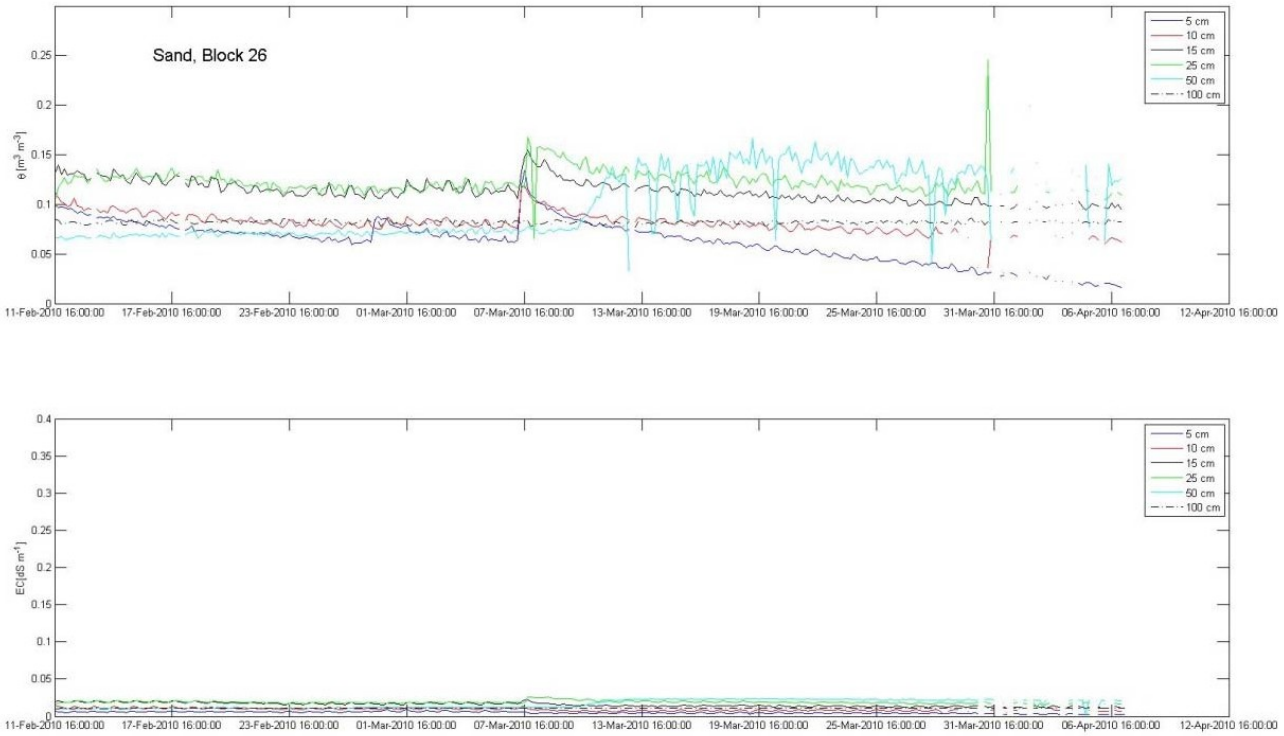

Figure 8. Time series of TDR-derived soil moisture (θ) and bulk electrical conductivity (EC) from block 26 in the sand plot.

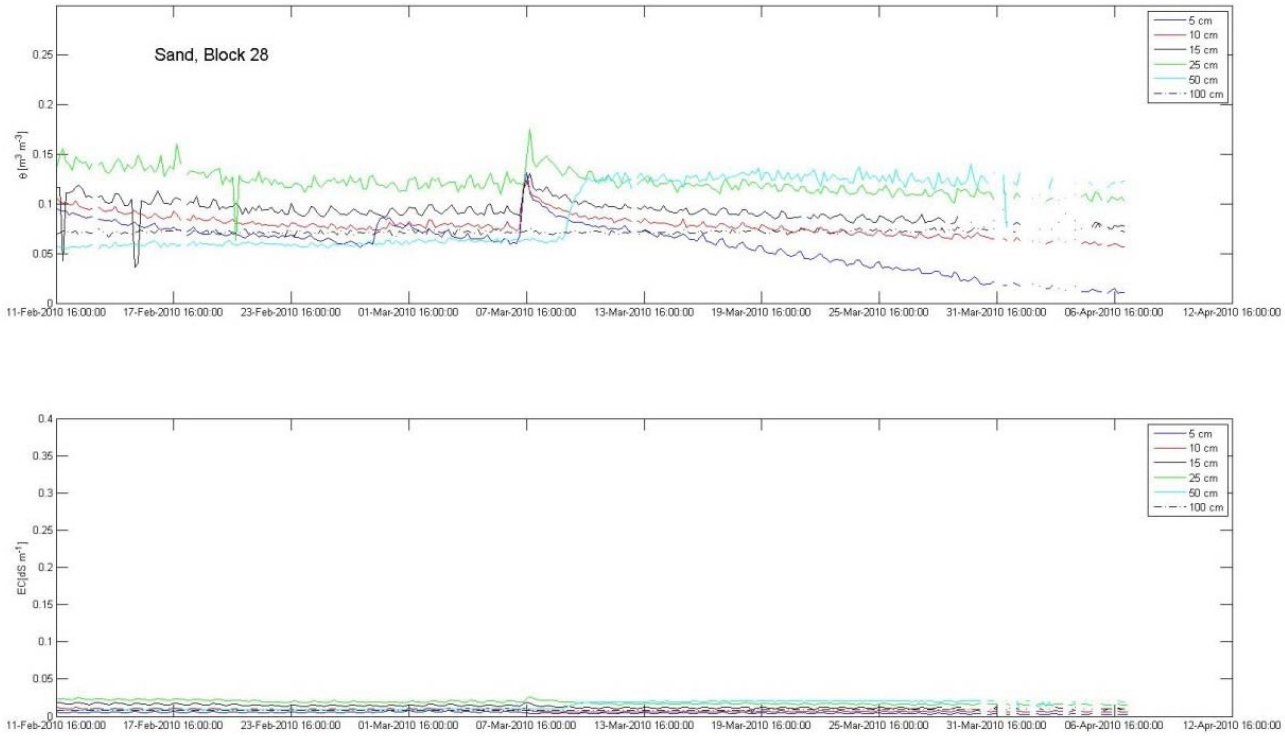

Figure 9. Time series of TDR-derived soil moisture (θ) and bulk electrical conductivity (EC) from block 28 in the sand plot.

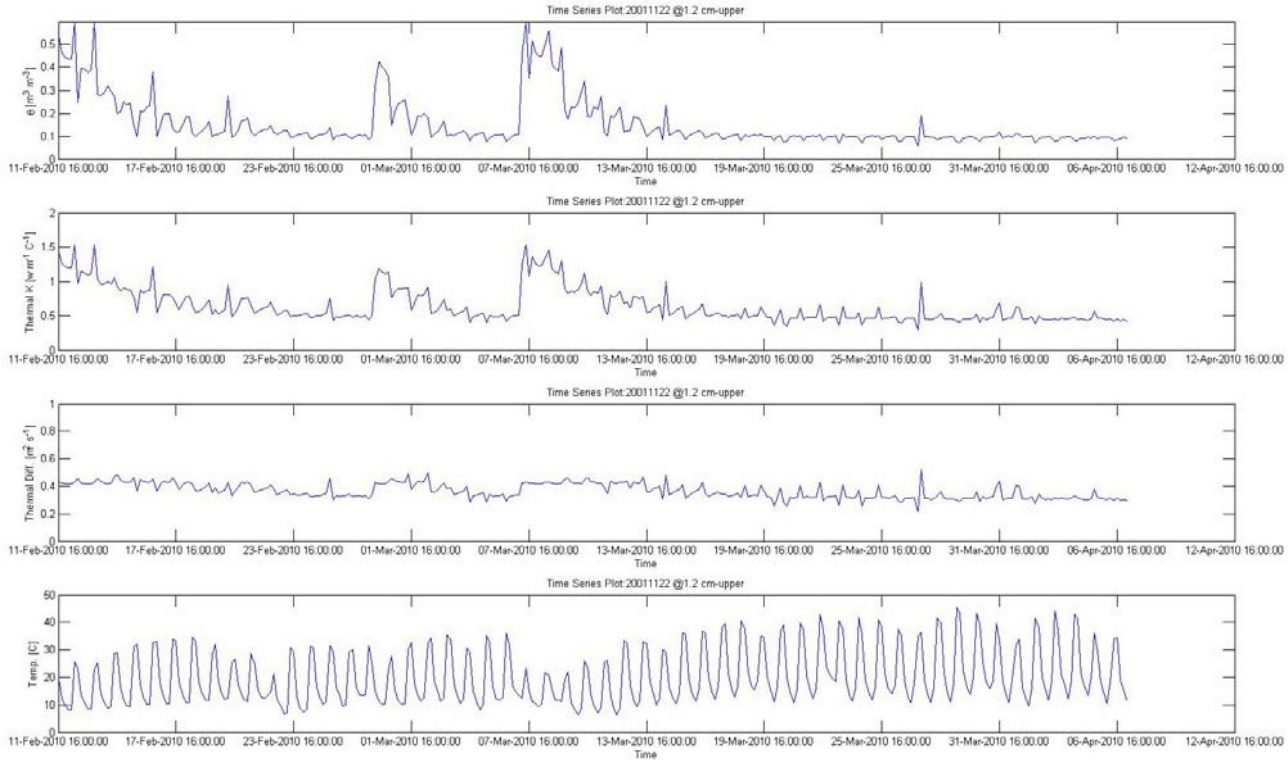

Figure 10. Time series of TPHP-derived soil moisture (θ), thermal conductivity (κ), diffusivity, and soil temperature at 1.2 cm depth.

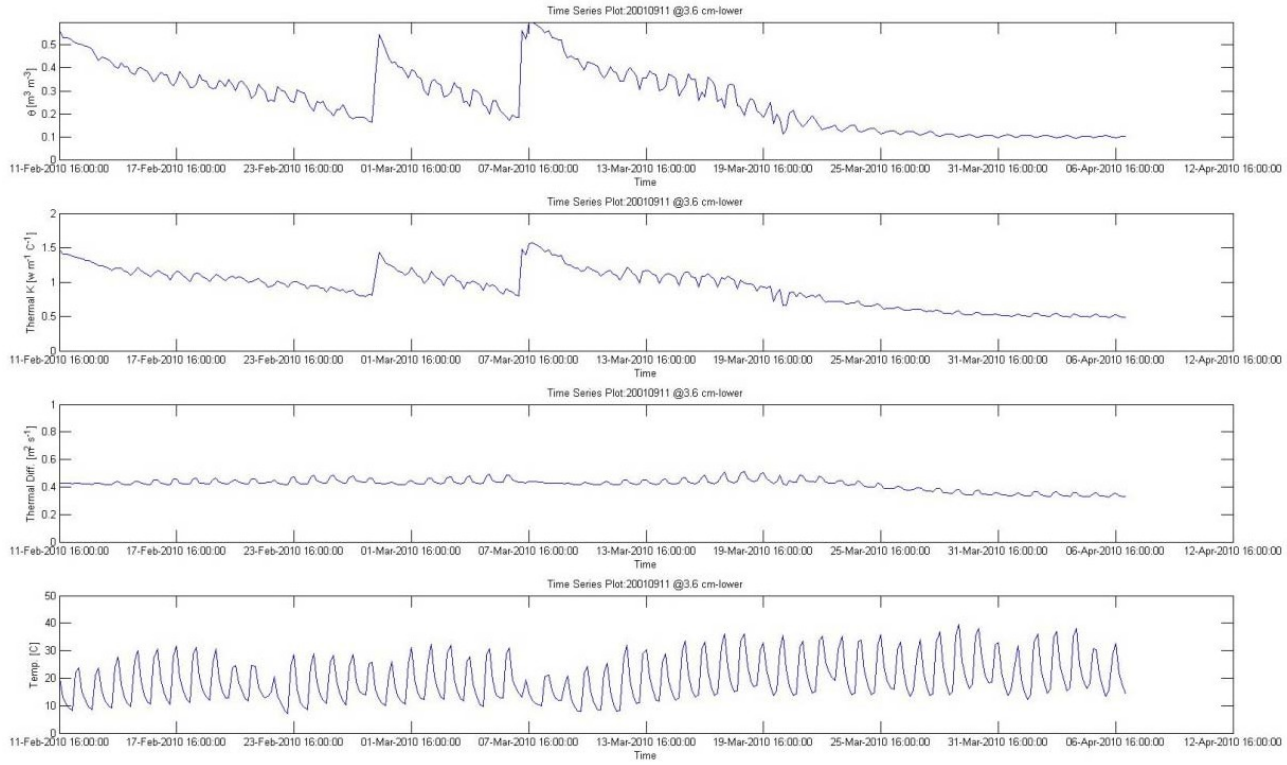

Figure 11. Time series of TPHP-derived soil moisture (θ), thermal conductivity (κ), diffusivity, and soil temperature at 3.6 cm depth.

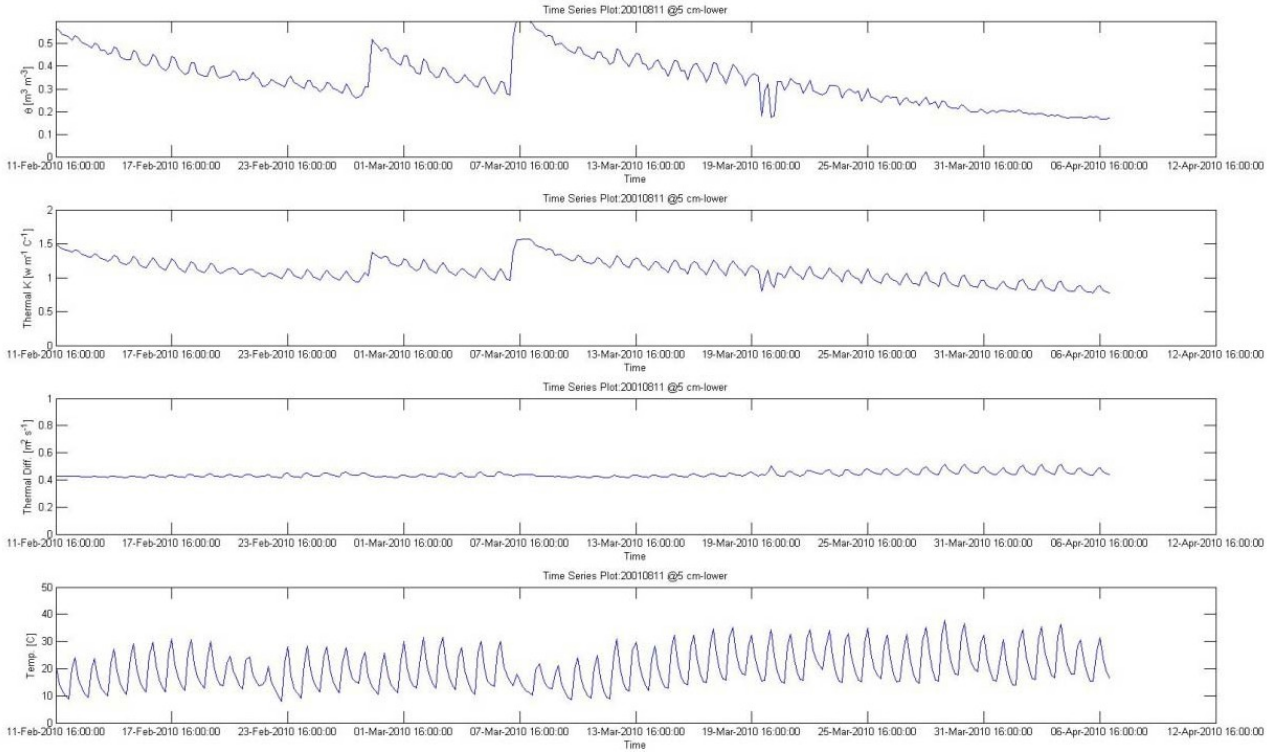

Figure 12. Time series of TPHP-derived soil moisture (θ), thermal conductivity (κ), diffusivity, and soil temperature at 5 cm depth.

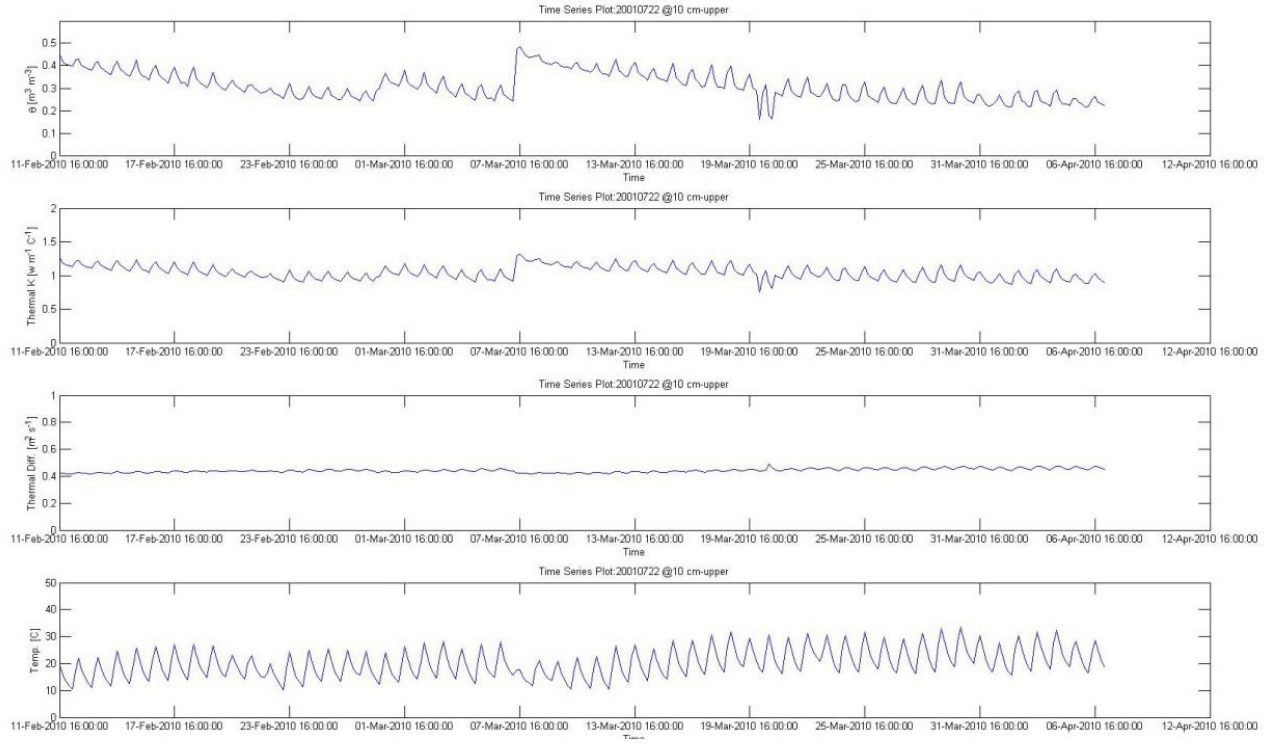

Figure 13. Time series of TPHP-derived soil moisture (θ), thermal conductivity (κ), diffusivity, and soil temperature at 10 cm depth.

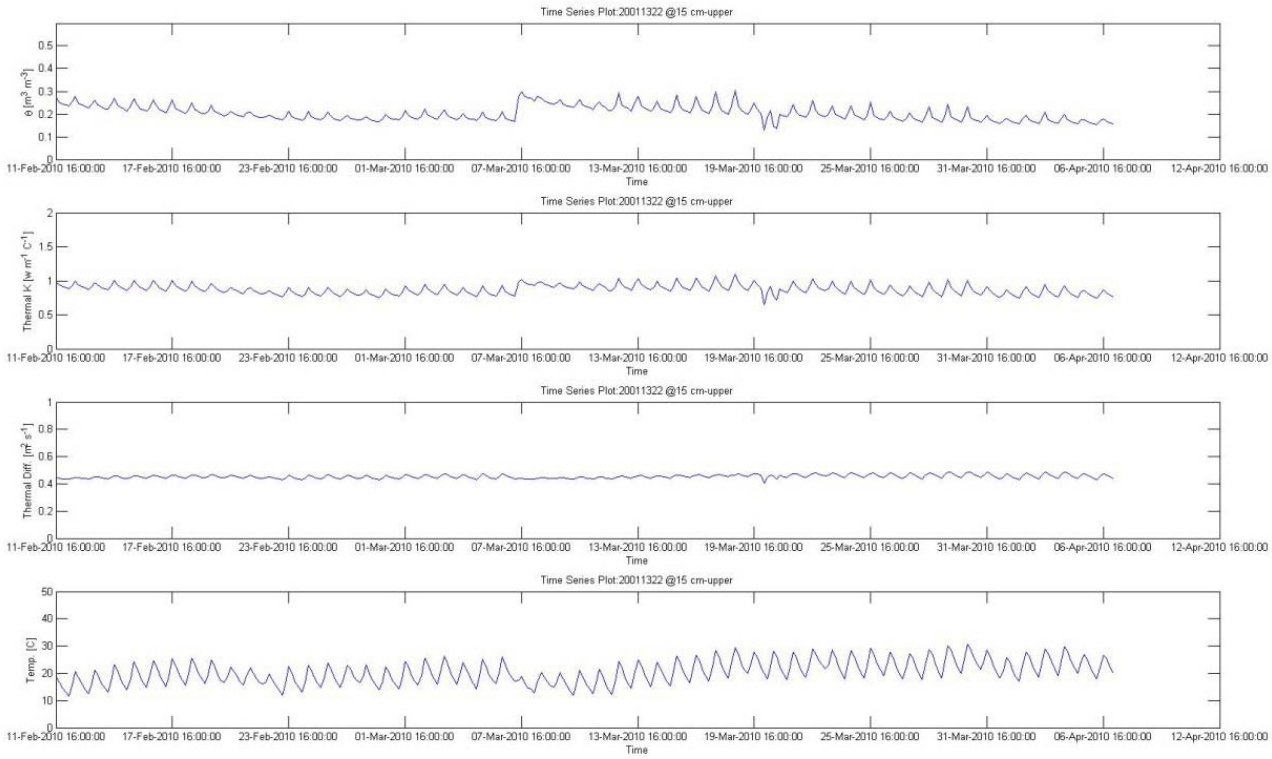

Figure 14. Time series of TPHP-derived soil moisture (θ), thermal conductivity (κ), diffusivity, and soil temperature at 15 cm depth.

The time-series data are collected in real-time at the Countermine facility, and are transmitted to DRI once per month. The series presented here covers only 11 February to 6 April 2010 - it serves only as an example of the data that can be and is being collected at each MERS site.

1.1.3 Desert Soil *In Situ* Monitoring at the Joint Experimental Range Complex (JERC), YPG

MERS Site Plan

Two master environmental reference sites (MERS) were established at the Joint Experimental Research Complex (JERC) site at YPG for comprehensive characterization and monitoring of soil variables, and evaluation of sensor technology. The two sites selected represent two extremes in the soils of the area: 1) a non-saline, fine textured soil (JERC-1); and 2) a hyper-saline, fine-textured soil (JERC-2).

The soils at each of the two MERS sites were fully characterized. Soil material was described and collected using traditional techniques of pit excavation, gridding, and description. Representative samples were obtained from each pit and analyzed for texture (including gravel), pH, carbonate content, and soluble salt chemistry. Of particular interest were the soil properties (e.g., clay mineralogy, soluble salt content, bulk density, and porosity) that vary among soil sites and how these properties may affect sensors, especially as related to changes in dielectric constant, magnetic susceptibility, and thermal conductivity.

At each site, an 8x8m area was marked as the primary study site within a much larger soil type area.

Within the 8x8m site, an automated monitoring system was deployed for *in situ* measurements of soil thermal properties (conductivity, capacity, and heat flux), electrical properties (dielectric permittivity and electrical conductivity), water content, water matric potential, and temperature. These measurements are made using a suite of thermal and electromagnetic (EM) based sensors buried to a depth of approximately 100-cm and controlled using CR10x data loggers by Campbell Scientific, Inc. (CSI). The general MERS site plan is shown in Figure 15.

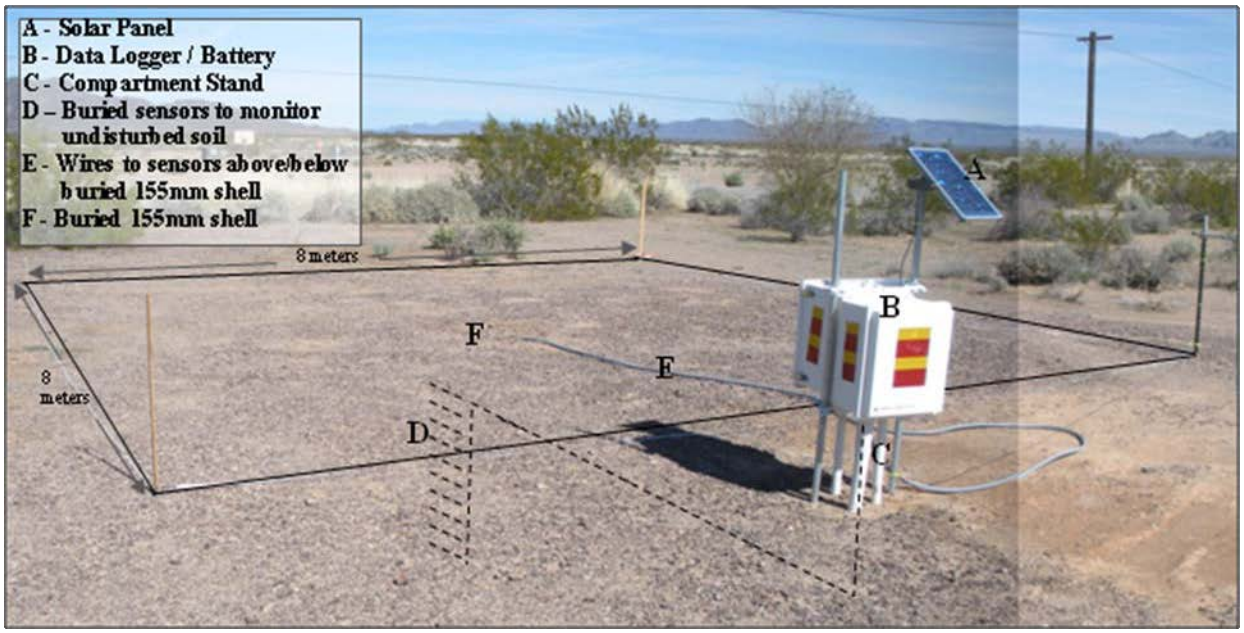

Figure 15. General MERS site plan shown over a photograph of the JERC-2 site. The dotted line indicates the location of the wires and buried sensors.

Results & Discussion

Although the soils at the two JERC sites are both fine-grained, they differ in their compositions and chemistry. Of the two, JERC-1 contains less gravel and sand and also has lower carbonate and salt contents. Also, JERC-2 has a thin desert pavement mantle not present at JERC-1. The presence of this mantle proved to have important consequences for soil moisture, permeability, and overall soil thermal properties.

The "dual probe heat pulse" (DPHP) and the "heat dissipation unit" (HDU) probes deployed at these sites provided excellent data, with the exception of a few spurious temperatures from the 10 cm DPHP sensor at JERC-1 and the 15 cm DPHP at JERC-2. Having redundant measurements from these two different sensors allows us to evaluate spurious values. As shown in Figure 16, soil temperatures measured by the two sensors are nearly identical. As expected, the near surface soil is subjected to greater fluctuations in temperatures, both diurnally and seasonally, than those at depth. Note that the temperatures at JERC-2 are higher than those at JERC-1. This is largely due to the thin desert pavement mantle that covers the surface of JERC-2, which is consequently darker than the JERC-1 surface. Diurnal temperature fluctuations are greatest at shallow depth (5cm), varying from ~20°C in the summer to ~10°C in the winter. At 60cm depth, the variance is only ~1.5°C in the summer and winter months.

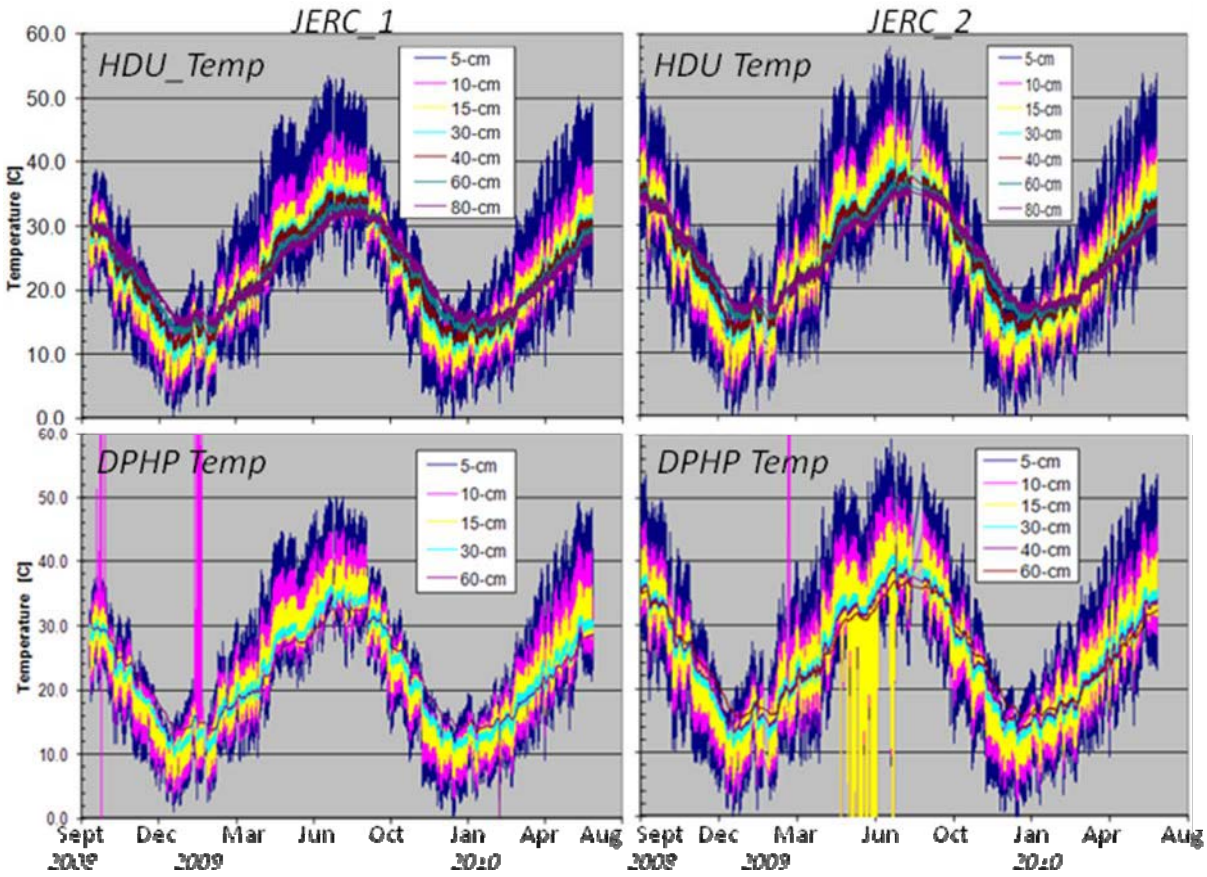

Figure 16. Soil temperature plots from both the DPHP and HDU sensors.

Soil water content, thermal diffusivity, and thermal conductivity, were measured by the DPHP probes (Figure 17). Results show that the thermal diffusivity and conductivity are closely connected to the level of soil moisture. The sudden inflections in the data are due to rainfall events (blue arrows) that occurred on the 11 September 2008, 26 November 2008, 16 December 2008, 7 February 2009, 3 July 2009, 9 September 2009, 11 December 2009, 2 January 2010, 24 January 2010, 2 February 2010, and 7 March 2010. The effect of rainfall on the soil moisture is greater at JERC-1 than at JERC-2. The compact soil and desert pavement mantle at JERC-2 appears to slow the infiltration of the rain into the soil.

Soil matric potential (Figure 18) is a measurement of soil pore pressure (related to moisture content, soil composition, particle size, and pore size.). The soil at JERC-1 – a non-saline, fine textured soil – has higher infiltration of rainfall at the near surface. This is expressed as strong inflections in matric potential during rain fall events in the 5 cm data. Much weaker inflections occur in the 5 cm data at JERC-2, where the soil is hyper-saline and fine textured, with a thin desert pavement. Soil matric potential is a measurement of ground-water movement potential and not of subsurface moisture.

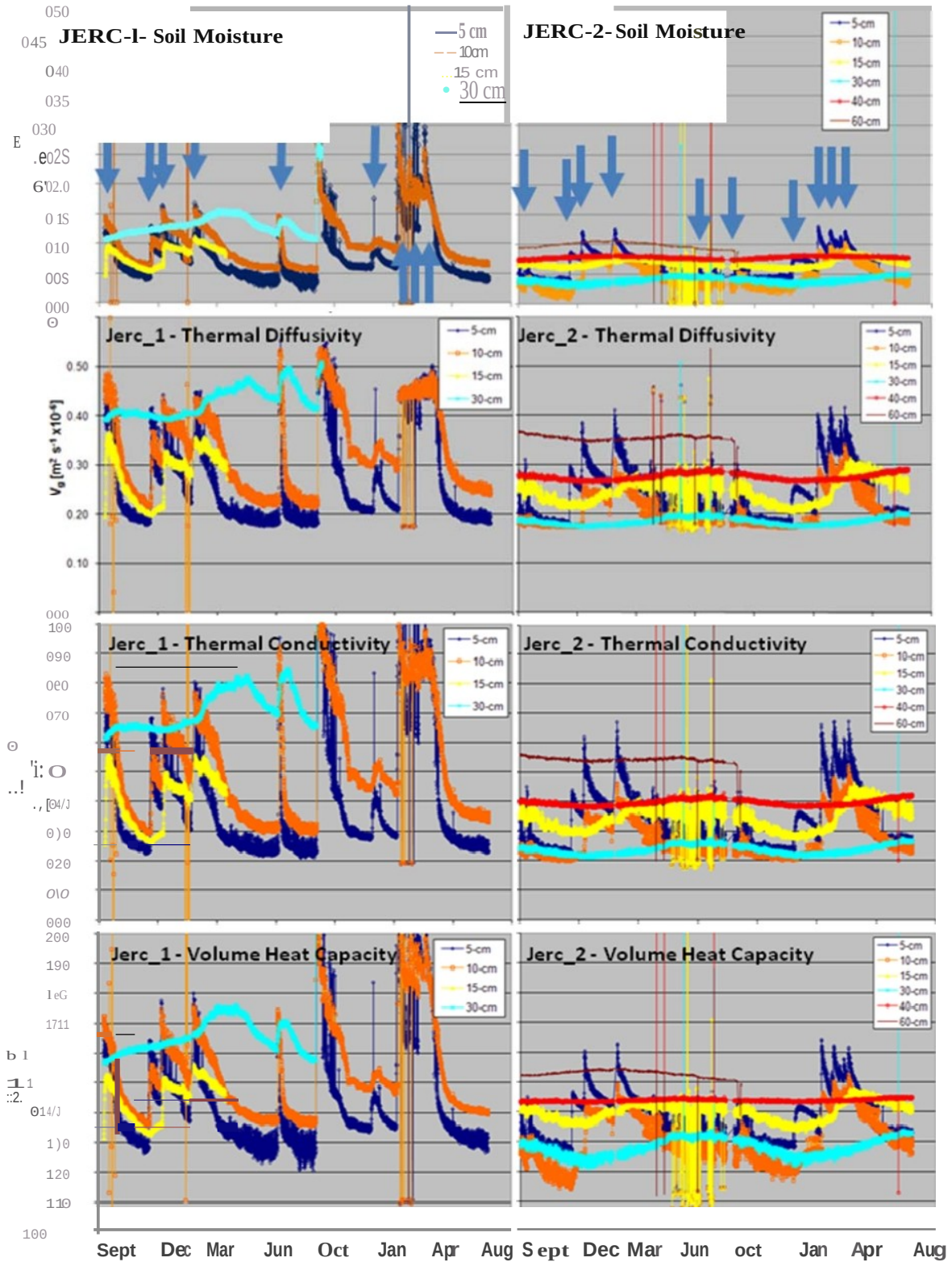

Figure 17. Soil water content, thermal diffusivity, and thermal conductivity measured by the DPHP (Dual Pulse Heat Probe) sensors. The blue arrows indicate rainfall events.

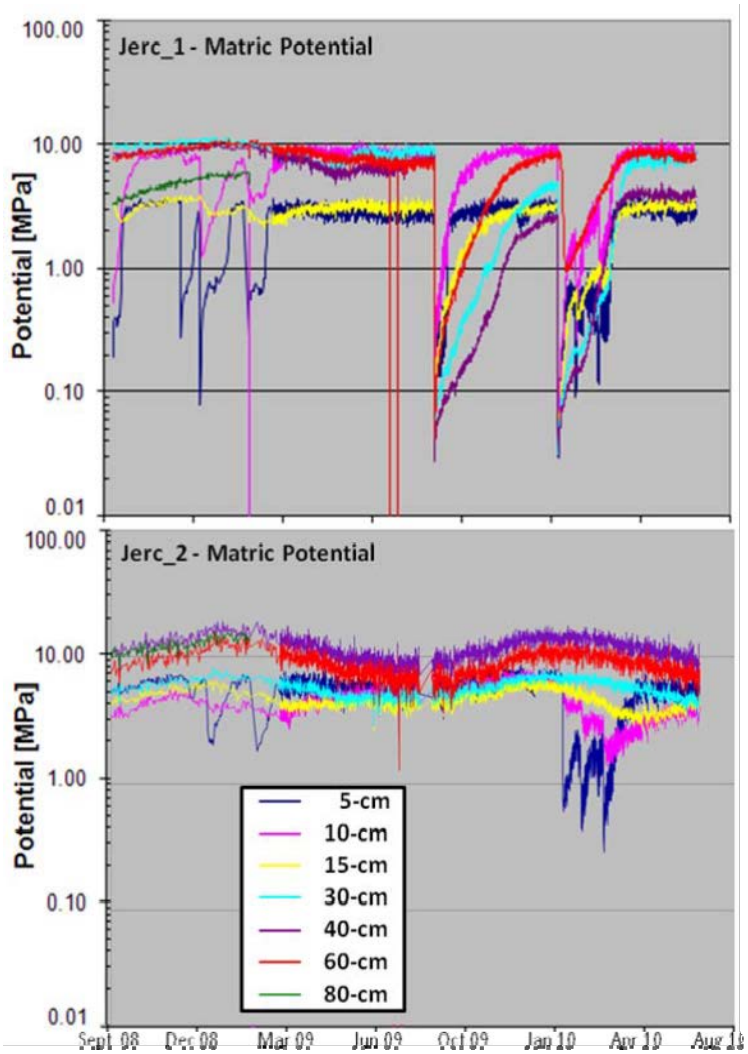

Figure 18. Soil matric potential plots for JERC-1 and JERC-2.

Soil moisture and electrical conductivity (Figures 19 and 20, respectively) were measured with the buried TDR (Time Domain Reflectometry) probes. The eleven TDR probes are buried at various depths, and operate by sending out an electrical pulse into the soil and measuring the change in the pulse from the surrounding soil. Soil moisture and electric conductivity are calculated from the measured signal using a program loaded into the data logger. Spurious spikes in the data are primarily due to the sensitivity of the program loaded into the logger being set too high in combination with the presence of an unknown electrical source (probably due to "classified" other work in the area). This was particularly an issue for the deeper probes. In December 2008, a new program was loaded into the logger to set the thresholds lower. Although this reduced sensitivity, it also reduced the noise in the data.

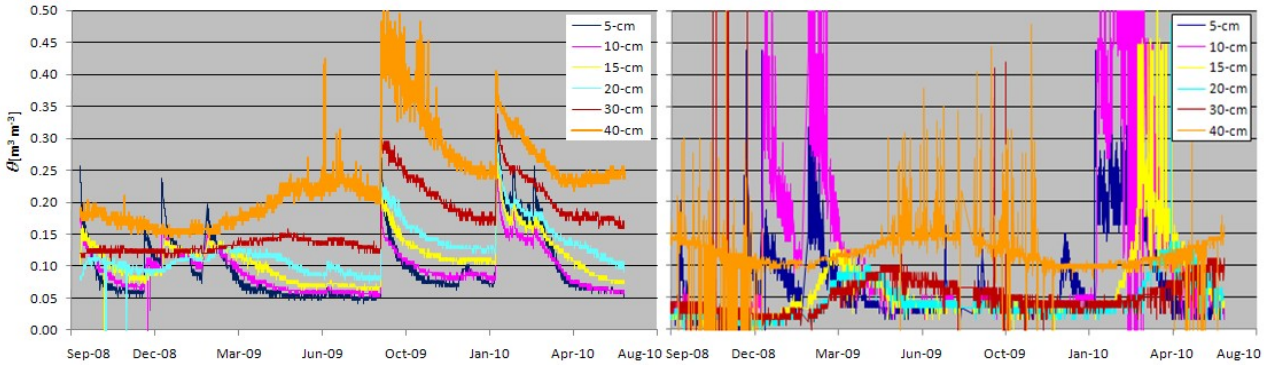

Figure 19. Detailed soil moisture plots for JERC-1 and JERC-2.

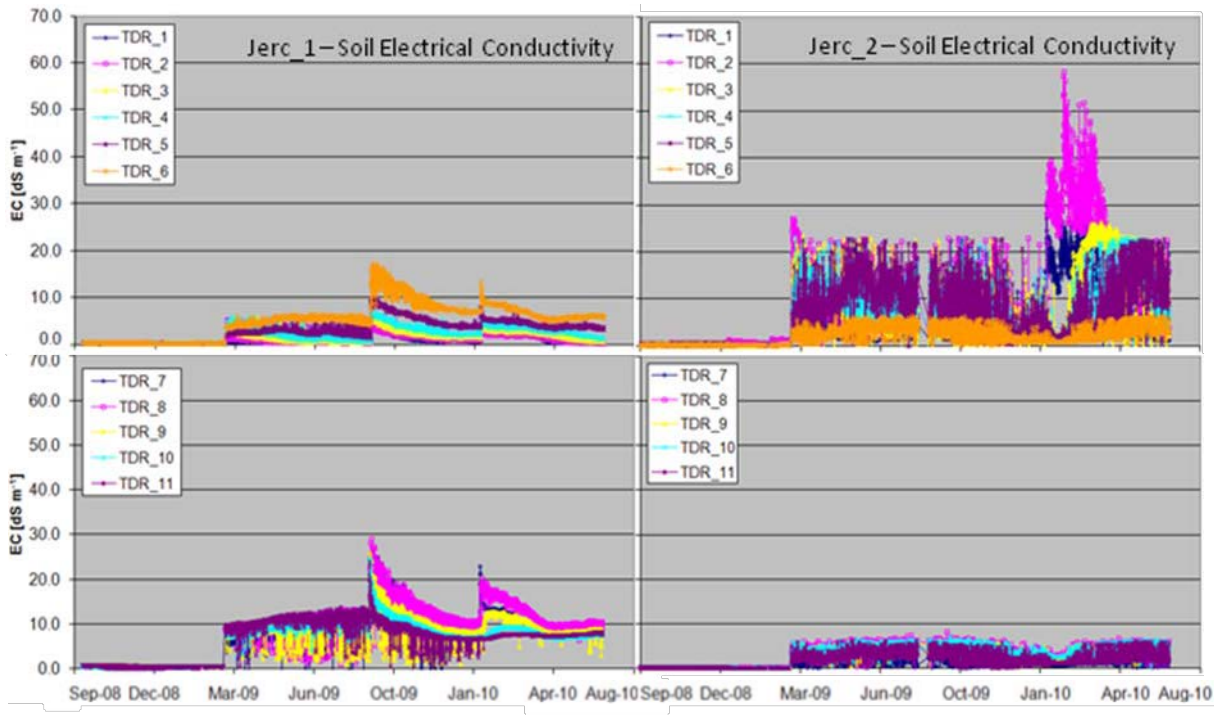

Figure 20. Soil electrical conductivity plots for JERC-1 and JERC-2.

JERC-1 is in general slightly wetter than JERC-2. The upper ~10 cm of both soils show distinctive TDR measured responses to rainfall that are similar to those measured with the DHP. The DHP measurements only go to a depth of 30 cm while the TDR goes to a depth of 95 cm. Seasonally, the soil was wetter in the fall and became drier during the winter (especially at depth). The electrical conductivity of the soil is similar for JERC-1 and 2 in the upper ~35cm; however, below that, it is much higher at JERC-1 than JERC-2. The higher soil moisture at JERC-1 undoubtedly has an effect here, and overrides the effect of the higher salinity at JERC-2.

1.1.4 Example of the application of MERS technology and methods in a hydrologic model study: Closing the Water Balance for Arid Soils – First Results from a Large Lysimeter Study, Boulder City, NV

Scaling the hydraulic properties of arid soils is problematic without full closure of the water balance. A recently constructed weighing lysimeter facility in Boulder City, NV (funded by NSF EPSCoR) provides an excellent opportunity to study water infiltration, storage, and evaporation in bare soils at the intermediate (meter) scale under well-defined boundary conditions. Three lysimeters are weighed on separate balances, each with a live mass of approximately 28,000 kg and a resolution of roughly 100 g or 0.025 mm of water. Each lysimeter contains 12 m^3 of repacked homogenized and layered desert soil (dimensions: 2.26 m diameter and 3 m deep) and is instrumented with 13 different sensor technologies to measure state variables including water content, matric potential, and thermal properties at 15

depth planes. A vertical rhizotron tube visually monitors movement of the infiltration front. Between July 2008 and 2011, 15 storm events were registered with the largest storm total yielding 62 mm of precipitation as well as snow (19-22 December 2010). By July 2011, there was nearly 350 mm of cumulative precipitation and the wetting front had reached 150 cm (Figure 21). This lysimeter facility fills a critical gap in our knowledge of the vadose zone hydrology of arid environments by closing the total water balance and providing discrete data on soil moisture redistribution in a 3 meter deep soil profile under well-defined initial and boundary conditions, allowing infiltration models to be evaluated and improved.

Technology transfer between this NSF-funded project and GMOE has created a collaborative effort in data collection, storage and visualization. Furthermore, numerical models developed under both projects have benefited from this full water balance closure, as well as lessons learned from sensors deployed prior.

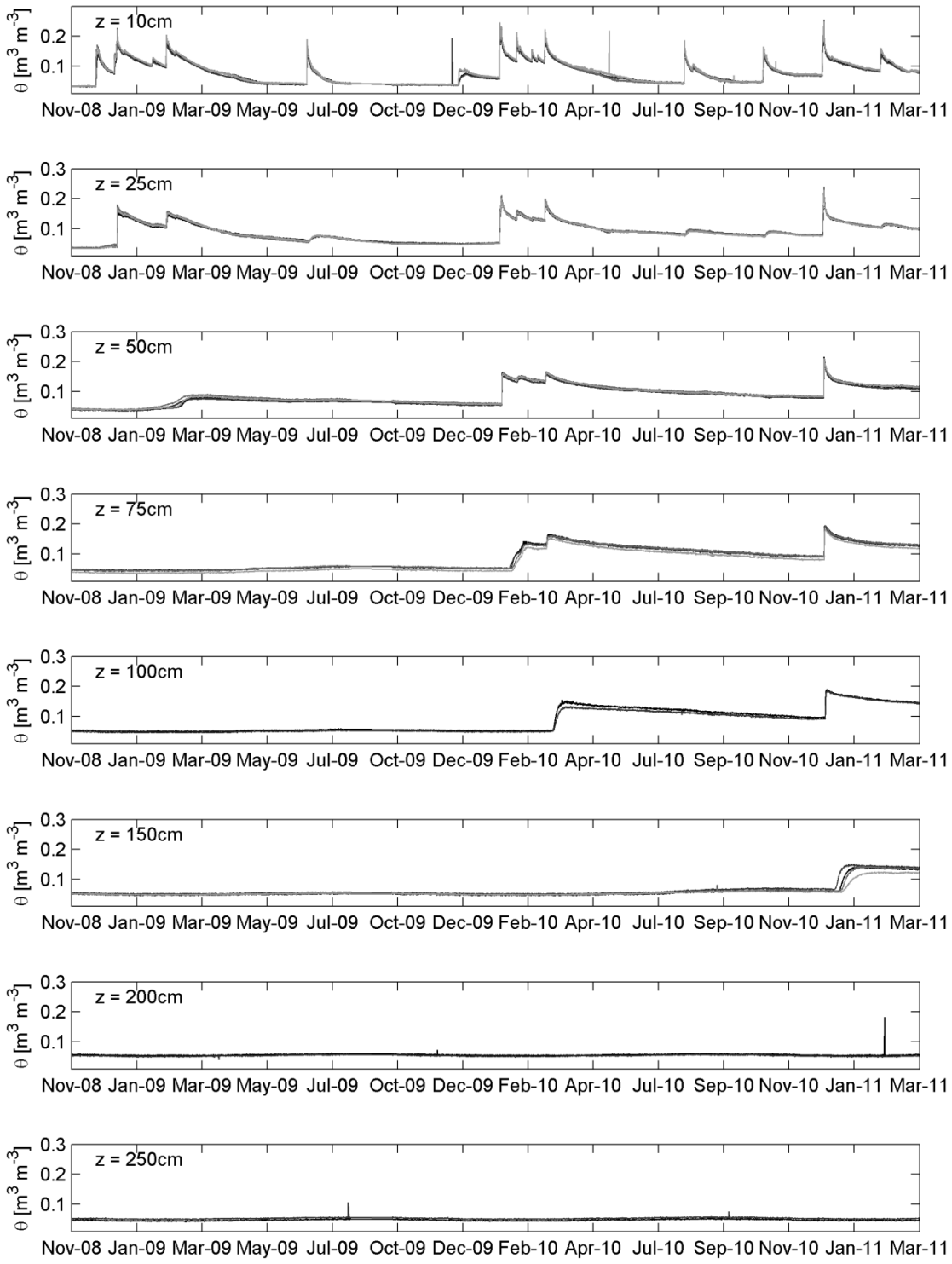

Figure 21. Replicated water content data (n=4) for the homogenized, disturbed soil in Tank 1 at the Boulder City lysimeter facility. The data show the wetting front arriving at 150 cm depth after nearly 30 months.

2. Detailed Analyses to Improve Understanding of Processes Taking Place within and Detection of Disturbed Soils in Support of Counter IED Technology

2.1.1 Analysis of thermal and electrical changes occurring in shallow soils following disturbance

In August 2008, we buried one 155mm inert shell at each of the two JERC sites. HDU (Heat Dissipation Unit) sensors were placed directly above and below the 155mm shells during a subsequent trip (9 –13 February 2009). These HDU sensors collect temperature and give a measurement of soil water content.

After the sensors were put in place around the buried inert shells, thermal FLIR (Forward Looking Infra Red) images were made at the JERC-1 and JERC-2 MERS. The plan was to record a thermal image every 5 minutes during a diurnal cycle at each site. The camera setup and an example of a FLIR image are shown in Figure 22. During the August 2008 site visit, time on site was limited due to local test restrictions; therefore, we were only able to record two hours of measurements at JERC-1 and 3.5 hours at JERC-2. However, during site visits in February and May 2009, we were able to make full diurnal measurements (Figure 23).

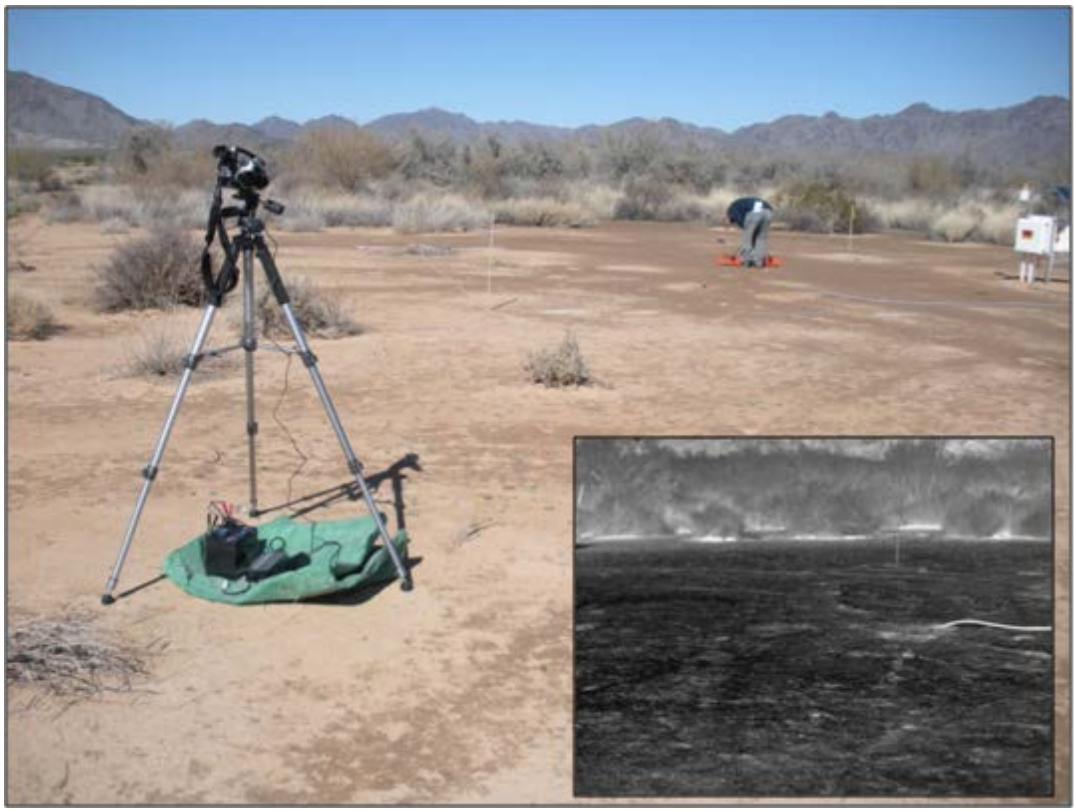

Figure 22. Thermal camera setup at JERC-1. The inset is a FLIR image of the site. The surface conduit containing the wires of the sensors above and below the buried 155 mm shell can be seen on the right side of the FLIR image.

Comparisons of radiant soil temperatures over/not over the shell made in February 2009 show that the temperature difference was never sufficient to allow detection at JERC-2; however at JERC-1, there may be adequate differences for detection during the day (Figure 23; upper graph). We speculate that this was due to the thin mantle of desert pavement at JERC-2, which obscures subsurface temperatures. The results from the measurements made in May 2009 are also shown in Figure 23 (lower graph). While in February, the soil above the shell was warmer than the surrounding soil by as much as 5°C, in May, the soil over the shell was slightly cooler during the day (+1°C), but slightly warmer at night (+0.2°C).

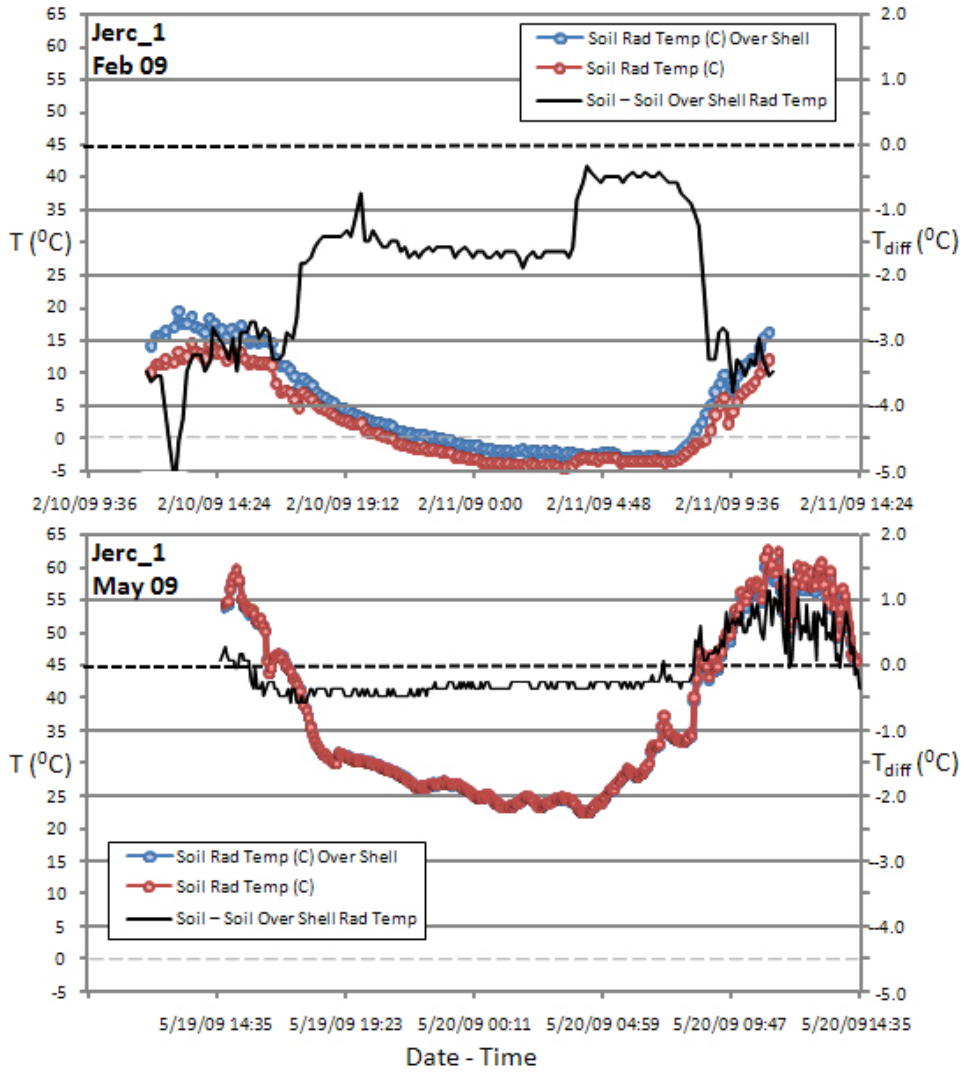

Figure 23. Soil surface radiant temperatures for soil over a buried 155 mm shell and undisturbed soil (no shell). These measurements were extracted from a sequence of FLIR images. The two sequences, made in February and May 2009, were ~24 hours long (5 minute intervals).

In terms of moisture status, the soil in immediate proximity to the buried shell was generally wetter than surrounding soil. Figure 24 is a plot of the difference in soil matric potential above and below the shell. Matric potential is closely related to soil moisture. The soil moisture above the shell responds rapidly to rainfall events (sudden upturn of the gray line (4 cm depth) on 06 July, 2009) but decreases slowly following the event, while soil below the shell tends to increase its water content slowly, and stay consistently wetter than soil at the same depth at a greater lateral distance from the shell.

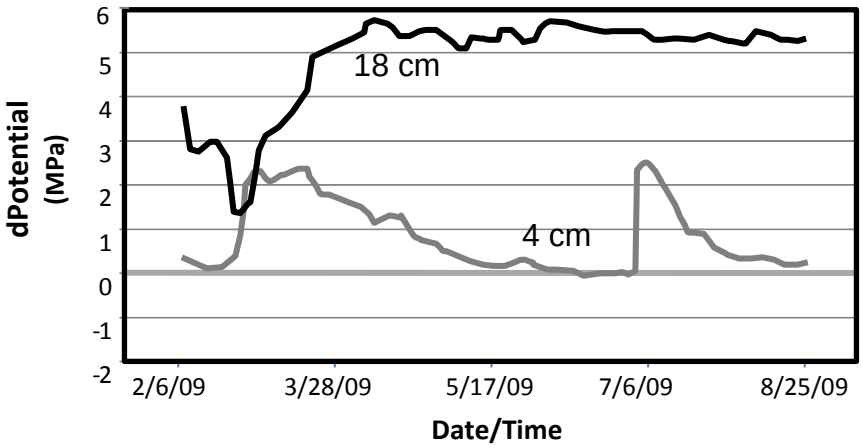

Figure 24. Differences in soil matric potential above and below a buried shell (4 and 18 cm, respectively). A higher matric potential indicates a wetter soil.

The use of Ground Penetrating Radar (GPR) to detect the buried inert round was also investigated at each site (Figure 25). This technology was indeed able to detect the buried shell; however, it should be noted that the rounds were buried after a rain event that had increased the subsurface soil moisture, and the soil immediately surrounding the shells likely became relatively dried out during the process of shell burial. Also, note that the ground penetrating radar was not successful in penetrating deeply into the hyper-saline soil (JERC-2) as compared to the non-saline soil (JERC-1).

The rain event that preceded shell burial is evident in the data-logged probe data as shown by the upturn in the lower two graphs of Figure 26. The data show that this particular rainfall event had a greater effect on the electrical and thermal properties of the hyper-saline soil of JERC-2, than those of the non-saline JERC-1 soil, at least at the 5 cm depth (~depth of the top of the shell). This may result from the presence of the well-developed desert pavement at JERC-2, which allows moisture to pool at the base of the mantle clasts, and slows down evaporation.

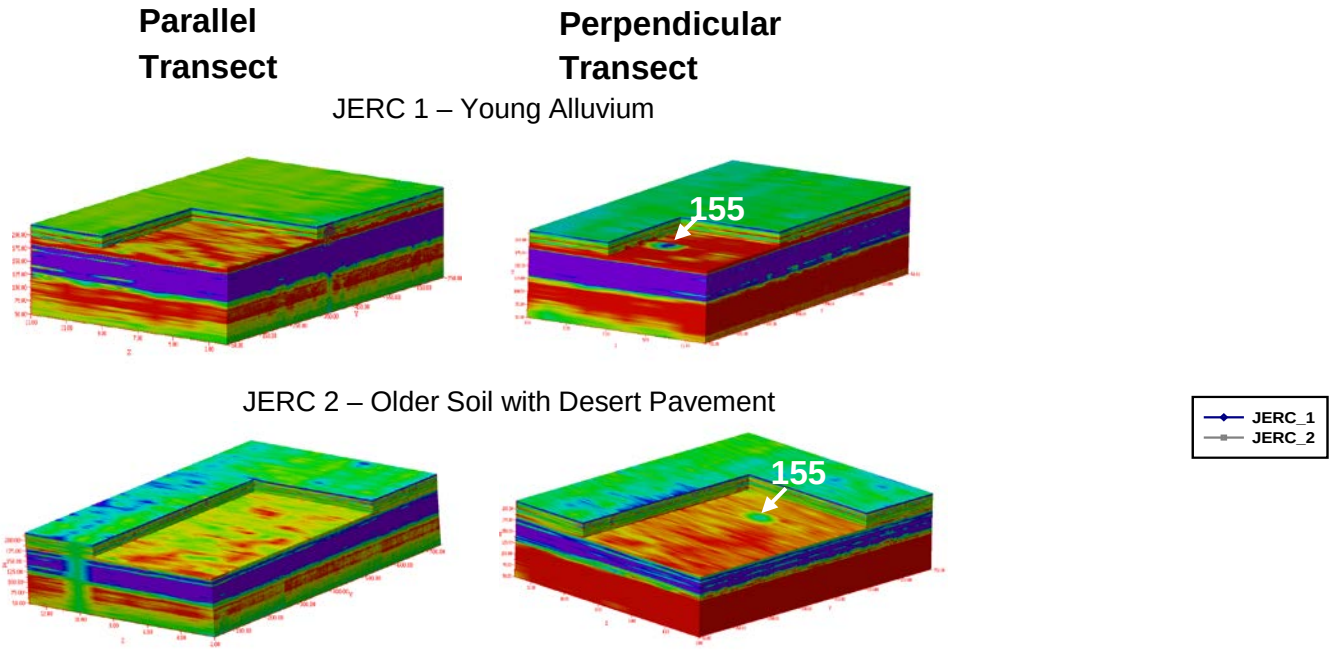

Figure 25. Ground penetrating radar (1000 MHz) grids over JERC-1 and JERC-2 taken on 28-29 August 2008 (shortly after the buried 155 mm shell was buried). The lack of GPR penetration into the lower subsurface at JERC-2 is due to the higher salt content at this site. Note the signal of the buried 155 mm shell at both sites.

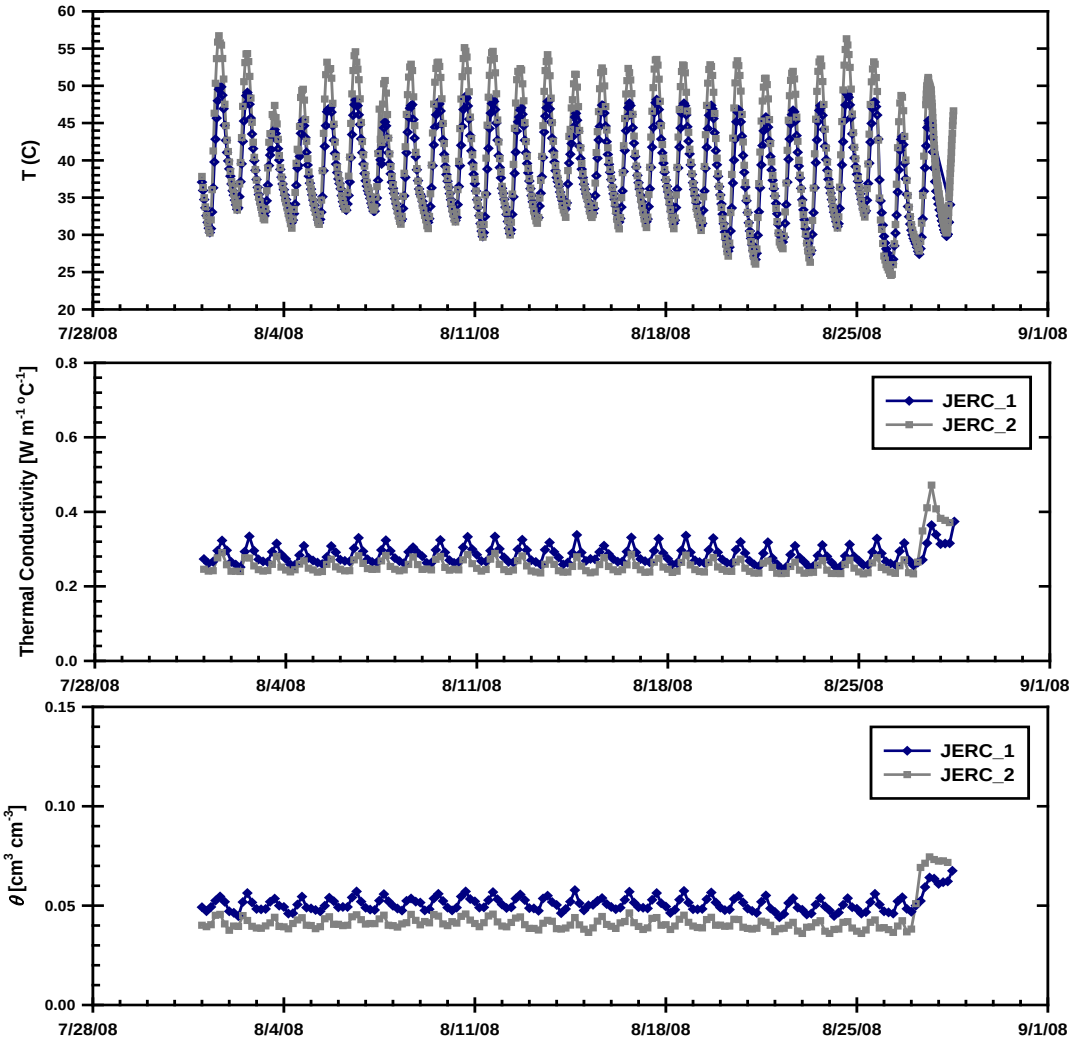

Figure 26. Comparison of the temperature, thermal conductivity, and soil matric potential at JERC-1 and JERC-2 (at a depth of 5 cm). The rainfall event on the evening of August 25 had a greater effect on the hyper saline soil (JERC-2) than the non-saline soil (JERC-1).

2.1.2 Evidence of soil structure formation in disturbed soils – numerical simulation and parameter optimization

Soil disturbance results in a structural disorganization of particles. Ultimately, the soil will return to a more ordered state over time, resulting in various changes to physical, mechanical and chemical properties that impact the distribution of soil moisture – a critical component of the bulk dielectric signature. The co-evolution of soil structure and hydraulic properties following disturbance were numerically simulated to better estimate the potential changes in GMOE MERS sites we may expect over the coming years and to discern if inverse modeling can obtain a robust and potentially dynamic parameter set after we have a sufficient time series. This task requires four steps to proceed for the forward simulation:

1. Generation of dynamic hydraulic properties over a range of textures and possible post-disturbance scenarios;
2. Generation of a stochastic climate covering a range of storm returns, depths, and evaporative demands;
3. Implementation of climatic boundary with evolutionary hydraulic properties in forward simulations to create the final time series of synthetic observational data;
4. Development of parameter optimization tools to allow for the dynamic properties and solve the inverse problem using observational data from step 3.

Forward simulations were conducted to generate a synthetic time series of soil moisture and temperature representative of two dynamic, post-disturbance scenarios: (1) settlement/consolidation and (2) formation of secondary porosity. Settlement and consolidation causes no change in particle size distribution but results in an increasing bulk density (decreasing porosity) with time. Hydraulic properties for this scenario were derived using the Rosetta Software (V2.0) and simulated for four soil types over a range of bulk densities from a non-compacted, disturbed value of 1.50 g cm^{-3} to a compacted value of 1.80 g cm^{-3} (Figure 27).

Secondary porosity (macropore formation) results from the formation of soil structure (reorientation of particles) following disturbance. A Durner-type bimodal porosity was assumed (Figure 28). Secondary structure ranged from 0 (black lines) to 50% (gray lines). The forward simulations drove the hydraulic properties forward (e.g. from black to gray) as a function of wet/dry cycle. Studies have documented a critical threshold at the plastic limit beyond which structural reformation is possible. Synthetic climates were developed to represent a range of potential climates for current and future MERS boxes. These served to drive the upper boundary of this model. The soil, represented by a series of 1-cm layers, began with homogeneous hydraulic properties (black line). Once the plastic limit was passed, the properties took a linear step forward and the simulation continued for some defined period of time. Once these forward simulations were completed, we began looking at the robustness of inverse solutions to this problem using multi-objective parameter estimation techniques.

Ultimately, the coevolution of soil structure and function will continue to be validated from real data obtained from the MERS boxes using in situ sensor data and geophysical methods. Laboratory experiments are also under way to investigate wetting/drying cycles on small cores.

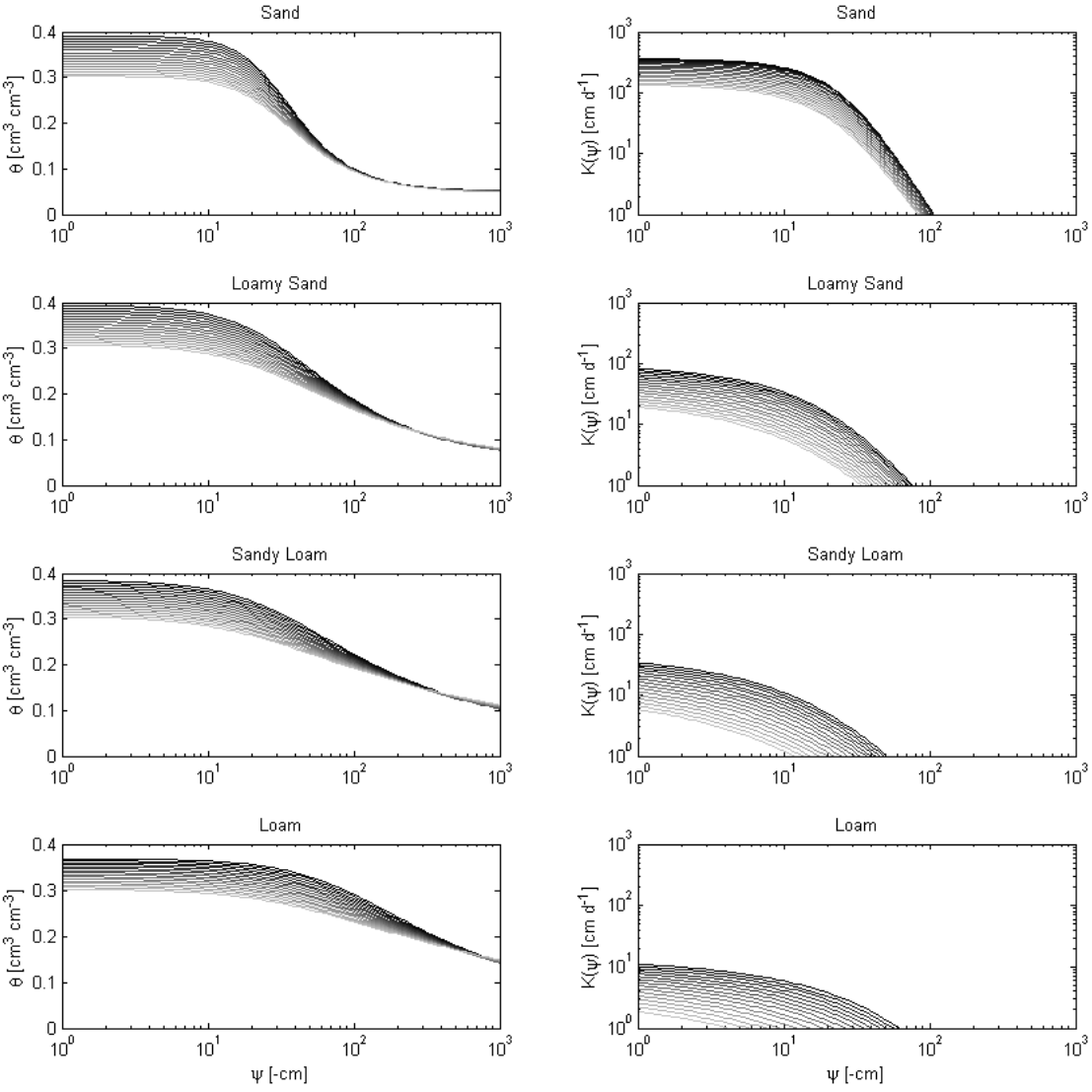

Figure 27. Consolidation effects on soil water retention (left column) and unsaturated hydraulic conductivity (right column) for four soil textures, with disturbed bulk density of 1.5 g/cm^3 (black) to a consolidated bulk density of 1.8 g/cm^3 (gray).

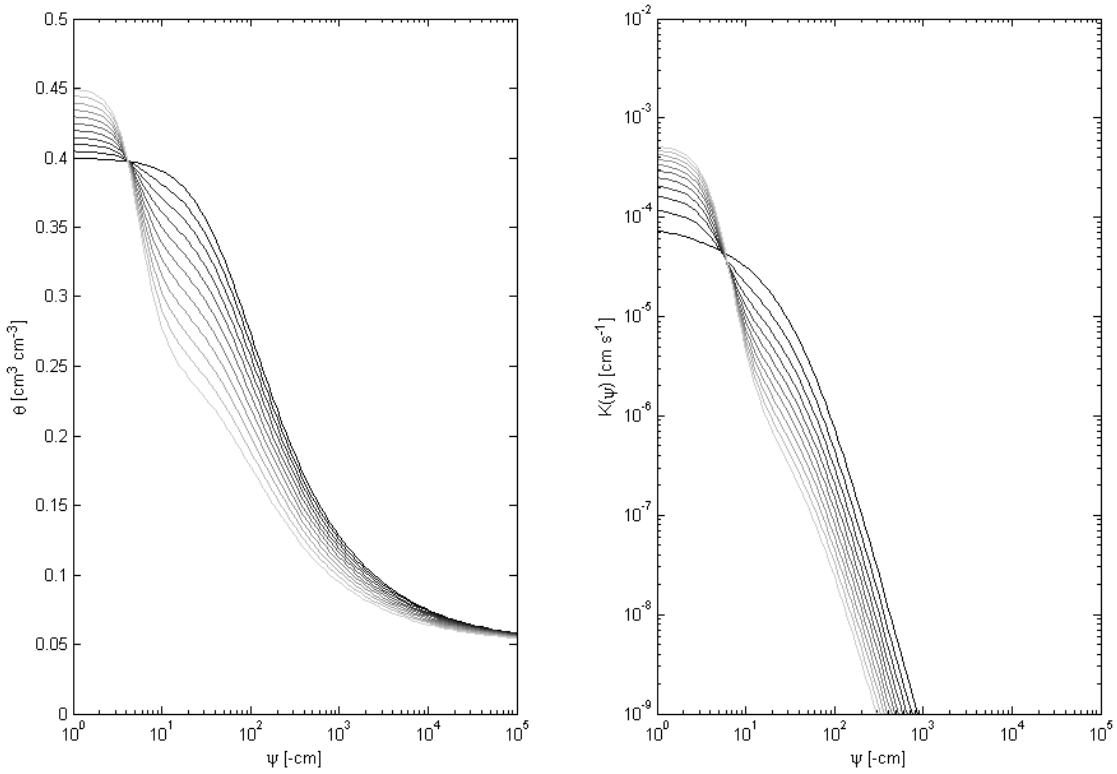

Figure 28. Durner type bimodality of pore-size distribution for the water retention function (left) and unsaturated hydraulic conductivity function (right).

2.1.3 The effect of bulk density on soil thermal properties

Thermal methods may prove to be useful in counter-IED technology. Soil disturbance such as that involved in IED burial alters the bulk density of the soil; and bulk density affects the grain-to-grain contact points that allow the transport of heat. Preliminary lab tests were conducted to examine the potential impacts of bulk density on thermal conductivity.

The original objective under the US Army Yuma Proving Ground (YPG) Soil-Air Geothermal Heat Exchange Test (SAGHET) (W9122R-07-C-0028) was to measure and characterize the basic soil thermal properties over a range of bulk densities and moisture contents. Soils samples were collected from four depths adjacent to soil thermo-exchanger trenches in February of 2010 and analyzed for physical, chemical, and thermal properties in the laboratory. In addition, similar analyses were conducted on alpha soil sites in both Iraq and Afghanistan for comparison to the YPG data. Results from the bulk density tests are summarized here.

Thermal properties were determined in the laboratory using the heat pulse method: A Triple Point

Heat Pulse sensor (TPHP) embedded in the test soil produces a heat pulse from the center needle and monitors the arrival of the pulse at the two exterior needles. It then solves the heat-flow equation to derive two measurements of thermal properties, the average of which was used in this case.

First, the fine-earth (<2mm) soils were packed into shallow (40mm) soil cells (Soil Measurement Systems, Tucson, AZ) with a diameter of 88mm (Figure 29). The cells were then saturated from beneath thereby minimizing any entrapped air. A Marriot system was used to supply water to the cell allowing it to infiltrate into the soil until the matric potential at the surface reached saturation (ψ = 0 kPa) (Figure 29[D]). This tension was maintained overnight to allow complete saturation of the soil matrix. The TPHP was inserted vertically into the soil cell and placed on to a recording balance. The data acquisition system (CR3000, Campbell Scientific, Logan, UT) was initiated and the Marriot supply disconnected. Laboratory air was blown across the top of the saturated cell which was subsequently allowed to evaporate. The TPHP probes made hourly measurement of thermal properties over a range of water contents (monitored independently from the recording scale using the hourly mean from 5-minute readings) as the water evaporated. Once the recorded mass returned to a value near its original, starting (dry) mass, the experiment was completed. The cell was emptied and the residual moisture content determined. The recorded mass was converted to volumetric soil moisture (ϑ) by correcting the final mass reading for the residual moisture and the total cell volume.

A total of six soils were evaluated. The primary soil excavated from 8' at the SAGHET demo site was packed to three different dry densities. Three soils from Iraq and one soil from Afghanistan were also tested at a single, moderately packed dry density. Lastly, the Ottawa 30-40 reference sand was tested to verify thermal property results.

The thermal properties were determined using the theoretical analysis of a fixed-width heat pulse (Kluitenberg et al., 1993; Das et al., 1995). The TPHP sensor consists of three 30 mm long needles separated by approximately 6mm. The heat pulse is generated by applying a precise voltage for 8s to the heater located in the center needle. The generated heat pulse is monitored at the two outer needles every 2s for a total of 80s after the heating time. The rate and magnitude of the heat pulse rise (dT) observed at some fixed radial distance (r) for the heater is a function of both the soil thermal capacity (C) and conductivity (λ) – both of which are affected by the volumetric water content (ϑ). By obtaining precise observations of $dT(t)$ at a known r, we can use parameter estimation to solve the heat flow equation.

The result of packing density is clearly observed in the thermal properties (Figure 30). Thermal conductivity (λ) increases with moisture, as well as with bulk density (Figure 30A). The ranges for λ are also presented in Table 4. Similarly, thermal diffusivity (κ) increases with moisture but tends to plateau around 0.10% (Figure 30B). The greatest difference in thermal properties between the different soil densities occurred at lower water content values; this could greatly aid detection technologies in the near-surface soil environment. Upscaling of this experiment is currently underway using thermal imaging technologies and wireless sensors at the NAES (Nevada Agricultural Experiment Station) MERS.

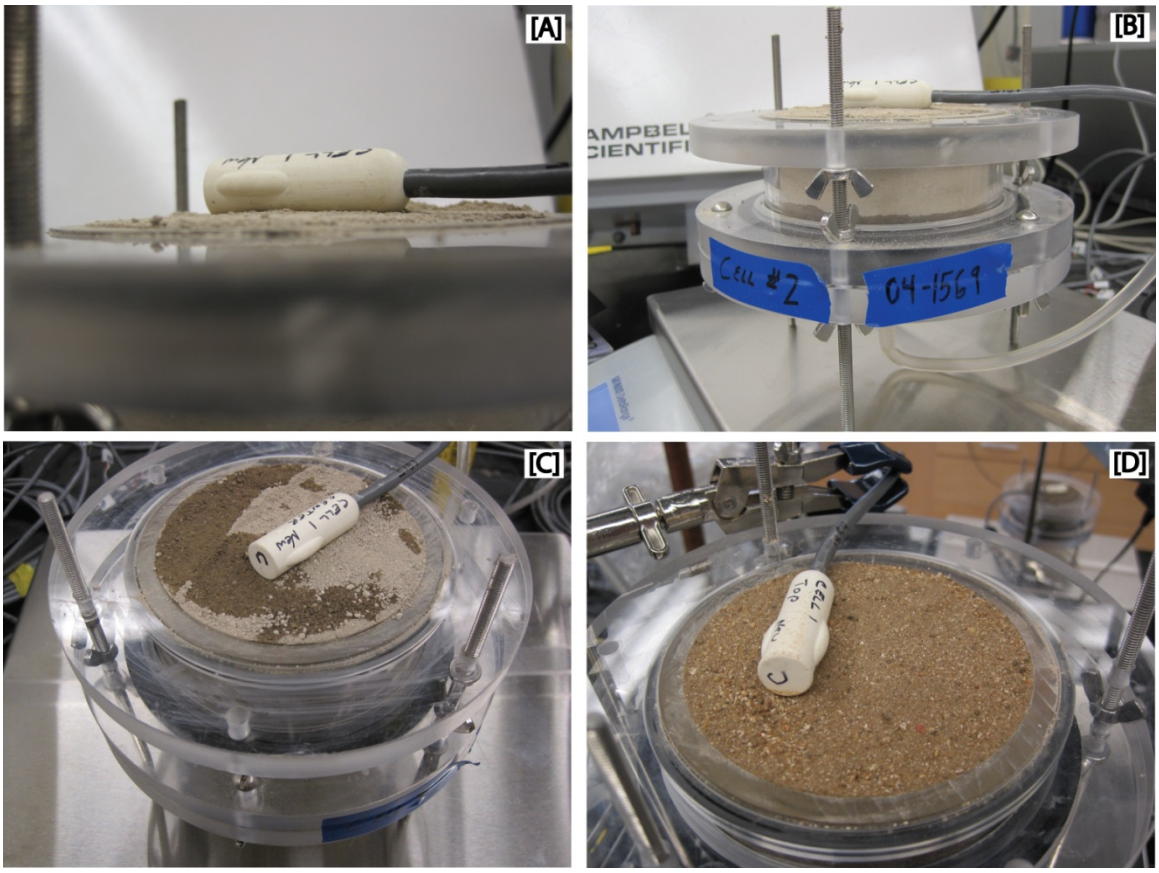

Figure 29. Experimental set up illustrating [A] the placement of the TPHP into the top of the flow cell, [B] upward filtration of water to saturate sample while on recording balance, [C] the surface becoming partially saturated, and then [D] fully saturated.

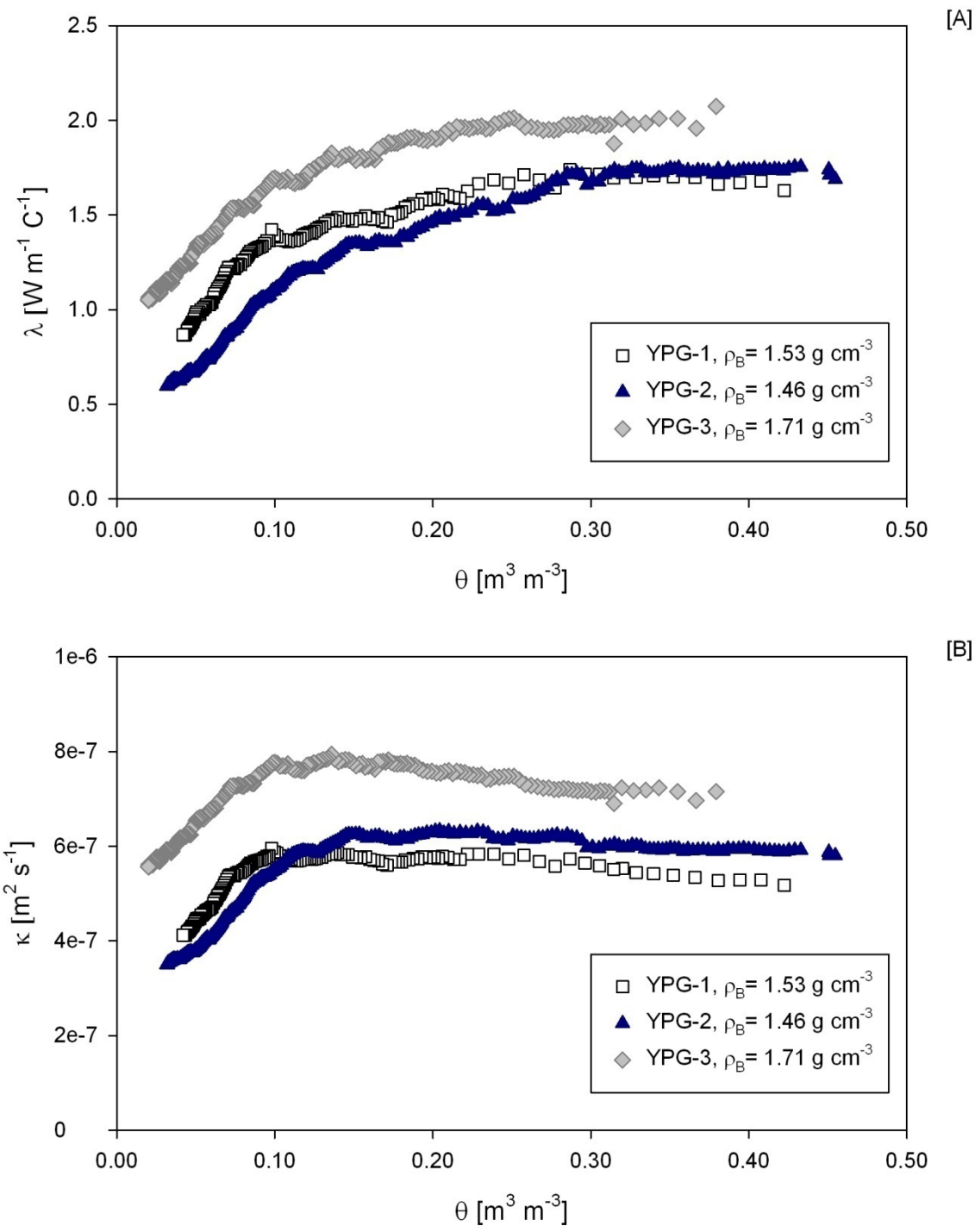

Figure 30. Results from evaporation experiments of the YPG SAGHET sample packed to three densities (ρB) for [A] thermal conductivity (λ), and [B] diffusivity (κ) as a function of moisture content (θ).

Table 4. Results from soil cells including bulk density (BD_{FE}), moisture content at saturation (θs) and residual (θr), and corresponding thermal conductivity at wet (λ_{wet}) and dry (λ_{dry}) ranges of moisture.

ID	Texture	BD_{FE}	θ_s	θ_r	λ_{wet}	λ_{dry}
		- g cm^{-3} -	- m^3 m^{-3} -	- m^3 m^{-3} -	- W m^{-1} C^{-1} -	- W m^{-1} C^{-1} -
YPG_1	loamy sand	1.532	0.422	0.042	1.906	0.864
YPG_2	"	1.458	0.455	0.032	1.754	0.595
YPG_3	"	1.710	0.379	0.020	2.073	1.048
04-1568						
Iraq 14a: Bulk Storage	sandy loam	1.678	0.409	0.055	2.461	0.779
04-1569						
Iraq 15a:						
Airport flood plain	silty clay loam	1.356	0.520	0.114	1.460	0.894
07-917:						
Khowst, Afghanistan	silt loam	1.588	0.534	0.004	1.841	0.547
07-921: Tikrit, Iraq	loam	1.407	0.460	0.058	1.625	0.464
NAES – GMOE Box	sand	1.540	0.402	0.003	1.727	0.328

References cited in this section

Das, B.S., Kluitenberg, G.J., and Pierzynski, G.M., 1995, Temperature dependence of nitrogen mineralization rate constant; a theoretical approach: Soil Science, v. 159, p. 294-300.

Kluitenberg, G.J., Sonon, L.S., Schwab, A.P., and Anonymous, 1993, Nonequilibrium adsorption and degradation of atrazine and alachlor in soil, Agricultural nonpoint sources of contaminants; a focus on herbicides: United States (USA), p. 20-20.

2.1.4 Light Detection and Ranging (LiDAR) Application for IED Detection and Microtopographic Surface Analysis

In late fall of 2009, GMOE personnel purchased a Leica Geosystems ScanStation™ II short-range terrestrial laser scanning system using internal funds provided by DRI's Division of Earth and Ecosystem Sciences (DEES). The system uses high resolution laser scanning technology (Light Detection and Ranging—or LiDAR) to survey microtopography and other geomorphological features (Figure 31). With a maximum, instantaneous scan speed of 50,000 points per second, full dome field-of-view, and excellent detection range (300 meters at 90% reflectivity), the system provides the capability to perform detailed topographic analyses of fans, desert pavements and other surfaces. A high-resolution internal digital camera aids with targeting and texture mapping of the scanned results. Along with the laser scanner, DRI also purchased a high speed laptop controller, as well as Leica Cyclone 7.0 software. The Cyclone software allows users to manipulate data point clouds and provides a number of processing options for three-dimensional scans.

Figure 31. Leica Geosystems ScanStation™ II at the 2C fan in the Cibola Range, YPG.

During late FY2010, the LiDAR was employed as an exploratory tool for the detection of wires of the type used by foreign combatants for IED detonation. This task incorporates analysis of surface microtopographic roughness elements due to their influence on wire detection. Yuma Proving Ground was selected for this exercise, as landforms in this area constitute important analogs for terrain in CENTCOM countries with active military conflict. The goal of this exercise was to determine if, and at what resolution, the LiDAR data will permit wire identification on desert surfaces of varying texture, disturbance, and topography.

Surfaces selected for this study included: 1) a sandy, active wash; 2) a cobbly to bouldery alluvial terrace with bar and swale morphology (Figure 32A); 3) an alluvial fan surface with a well-developed desert pavement and thick dust cap, severely disturbed by human activities; 4) a gravel road surface with a high potential for dust production (Figure 33A); 5) a series of gravel-mantled badland hillslopes; and 6) a man-made sand test course representative of a sand sea/dunefield. These landforms

comprise analogs to surfaces present in Afghanistan, and to a lesser extent, in Iran, Iraq, Israel, Jordan, Pakistan, and Syria.

A series of eight wires of progressively finer gauge were stretched at 18-inch intervals between 1-inch diameter wooden poles and laid over the ground surface to simulate the types of wires that might be employed for IED detonation. Because this exercise constituted an exploratory test of the laser scanner to detect these wires, no attempt was made to actively camouflage them. The LiDAR was used to scan the wires at both extremely high (5 mm) and moderate (5 cm) point densities. Laser scanning datasets collected from various angles at a single site were reconciled together and rendered visually in 3-dimensional space in a software program called Cyclone (Figures 32B and 33B) upon fieldwork completion. This allows the user to view the data and select areas of interest, but has limited capabilities for data analysis in terms of our microtopographic surface characterization objectives.

Detailed microtopographic measurements made possible by LiDAR measurements are unparalleled when compared against traditional field-based surface characterization methods. The power of the LiDAR for topographic analysis is the ability to represent microtopographic features in a digital dataset with a basic (x,y,z) 3-D format, each point coupled with a measure of laser intensity return (surface reflectance). A single scan of a small (<400 m^2) area may produce >15 million individual point measurements. However, at present there is no standard processing method for handling datasets of this magnitude available in the geostatistical scientific community; data analysis methods are typically defined by the user for specific products as directed by the research objectives. Currently, using readily-available toolsets, we are able to render unprocessed datasets for rapid scene visualization and manual identification of coarse-gauge (> 2mm diameter) wires, using the combination of Cyclone and ArcGIS® (ESRI®) software, coupled with a free data processing and filtering utility for digital elevation model production, GEON points2grid (Active Tectonics Research Group, Arizona State University), developed with funding from the National Science Foundation. Figures 34 and 35 show examples of a detection dataset rendered using different techniques. The footprint of the laser on the landscape (approximately 2 mm at decimeter-scale ranges) precludes identification of the thinner, single-gauge wires in these visualizations.

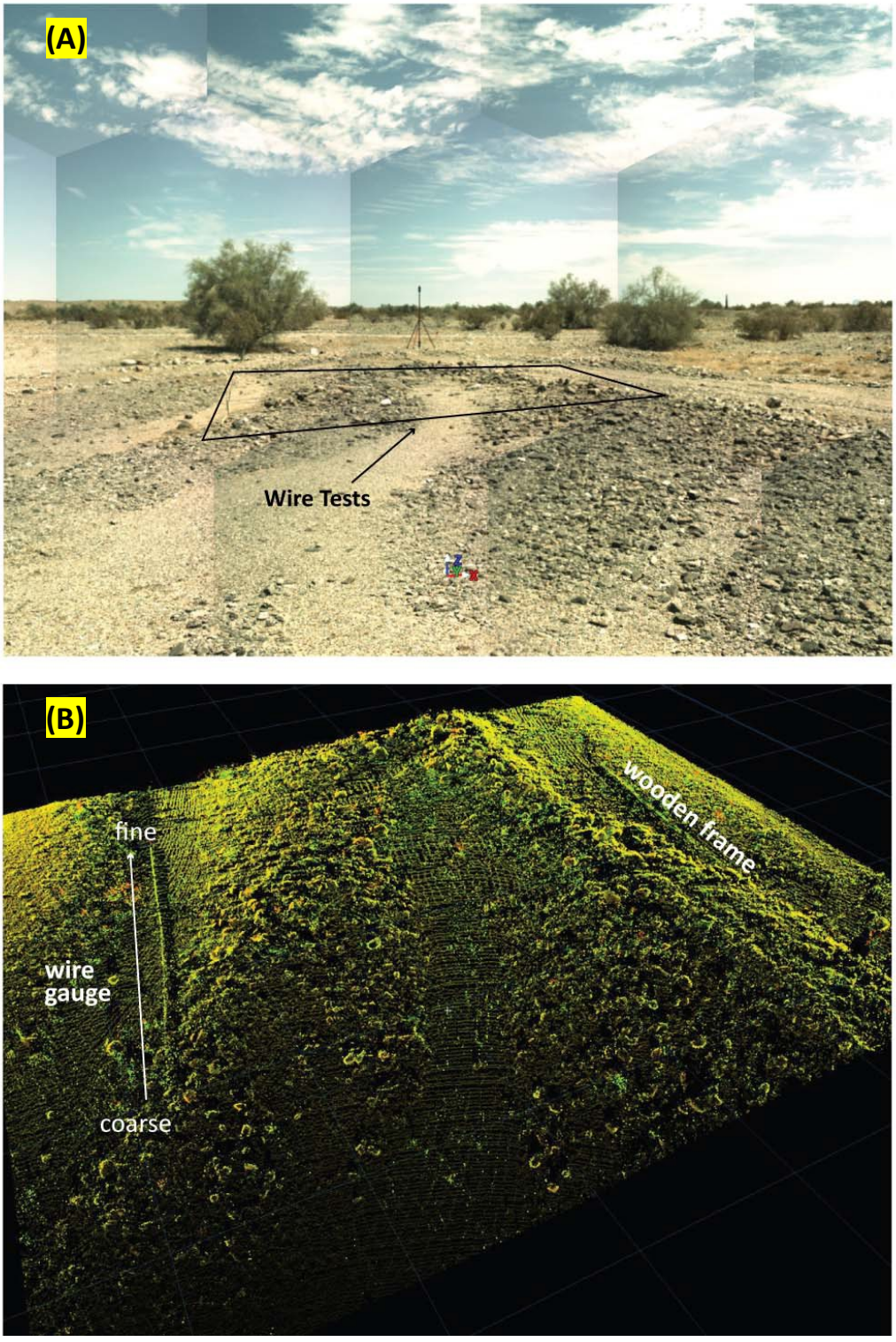

Figure 32. (A) Photomosaic of the cobbly alluvial terrace at YPG, taken using the 360˚ high-resolution camera integrated into the LiDAR unit, showing where the wire detection test was conducted. (B) 3-D visualization (colored by laser return intensity) of the wire test. Only the frame for the wires appears in the scan, as the coarseness of the surface camouflages the wires.

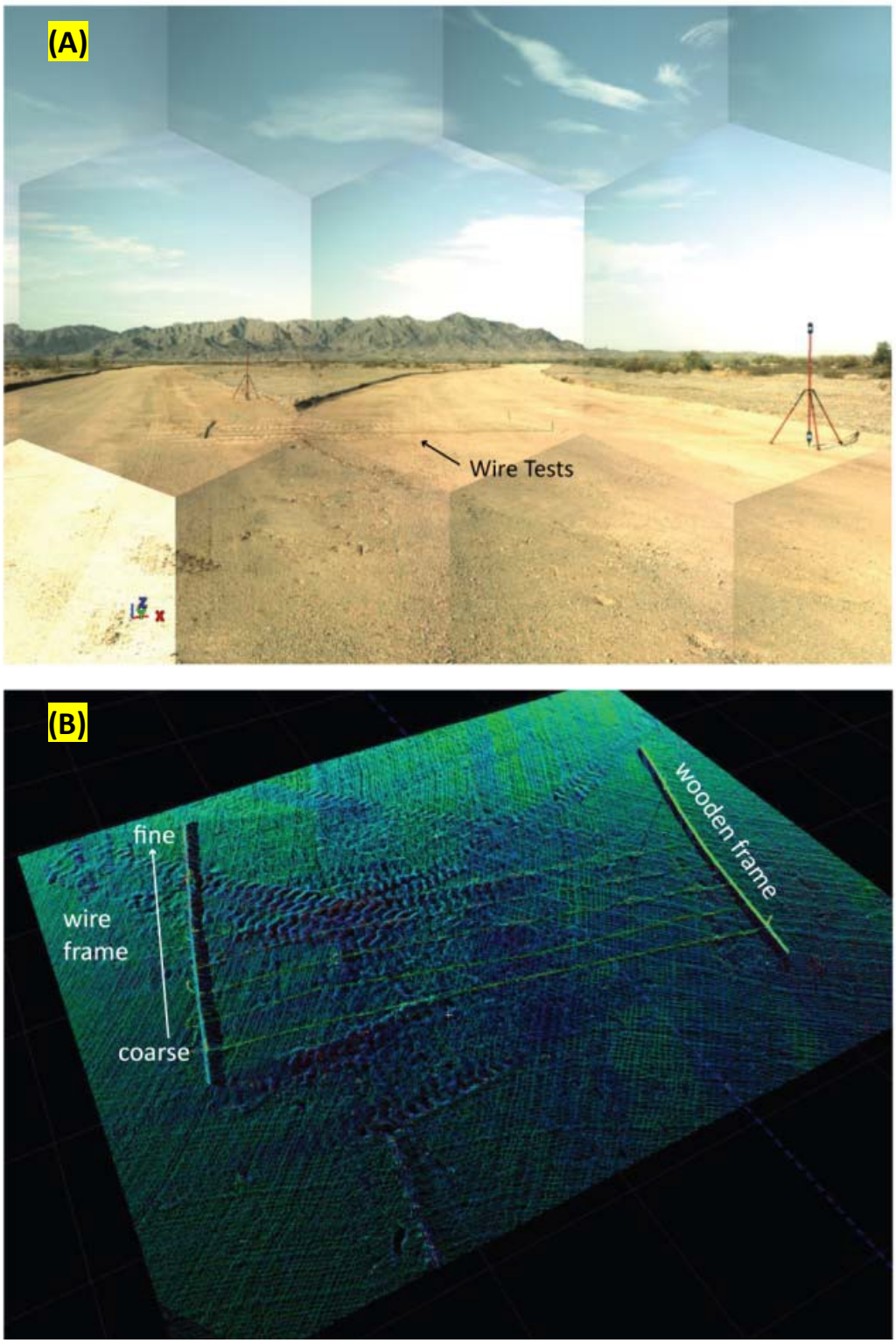

Figure 33. (A) Photomosaic of the gravel road with high dust content, showing where the wire detection test was conducted. (B) 3-D visualization (colored by laser return intensity) of the wire test. Limiting the stretched color range in this scan allows the coarse-gauge wires to become clearly visible, which is made easier by having them overlain on a smooth surface.

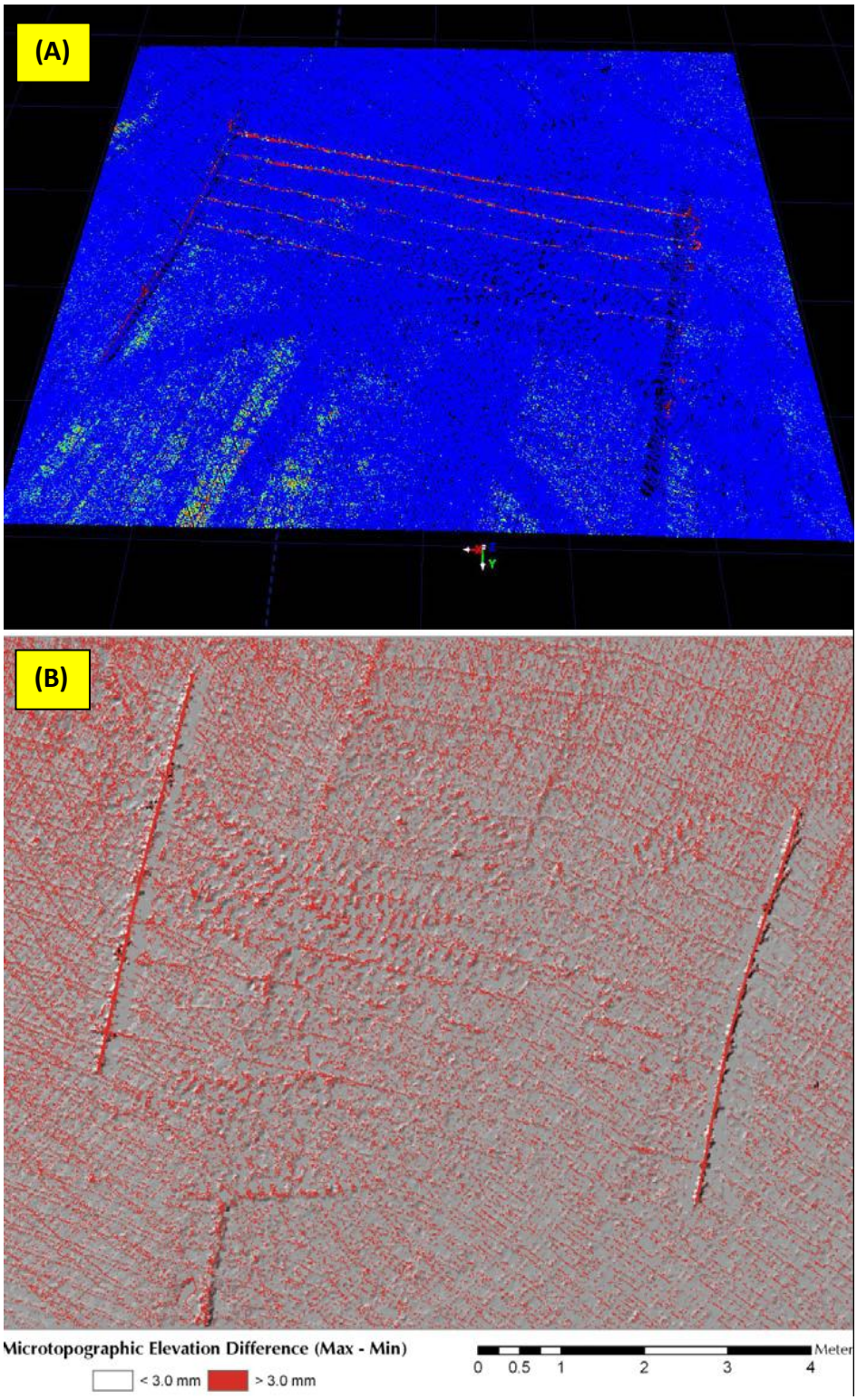

Figure 34. (A) Manual wire isolation using the visualization tools in Cyclone, made possible by limiting the colored representation of laser return intensity to values that closely flank the reflectance value of the wires. In this manner, the wires lie at one end of the spectrum, while all higher values are represented by a distinctly different color. (B) Manual wire isolation using surface elevation by exporting point cloud data to GEON points2grid, and creating a continuous raster surface. With this tool, wires can be isolated by elevation relative to the underlying surface, but only for very smooth surfaces. Interference relating to the path of the laser itself—as well as microtopographic elements like tire tracks—makes this method less useful.

Ongoing work at DRI includes investigating existing analytical algorithms for surface visualization and textural analysis, and initiating development of new algorithms in MATLAB® (MathWorks™) for processing the ScanStation II point cloud data outputs from Cyclone. Figure 35 shows an example of a MATLAB-produced LiDAR visualization, showing the detail available for surface roughness analyses. Although, this has not been repeated yet with LiDAR thinwire datasets, exploratory work with MATLAB to date indicates that it provides a more robust method with a high level of user control for isolating the wires from the original, high-resolution scans, as well as quantifying surface roughness of the wire detection test environments. Roughness statistics will help determine the influence of the ambient topographic noise (e.g., surface topographic variability, shadows in scan field-of-view, concealment by vegetation) on wire detection.

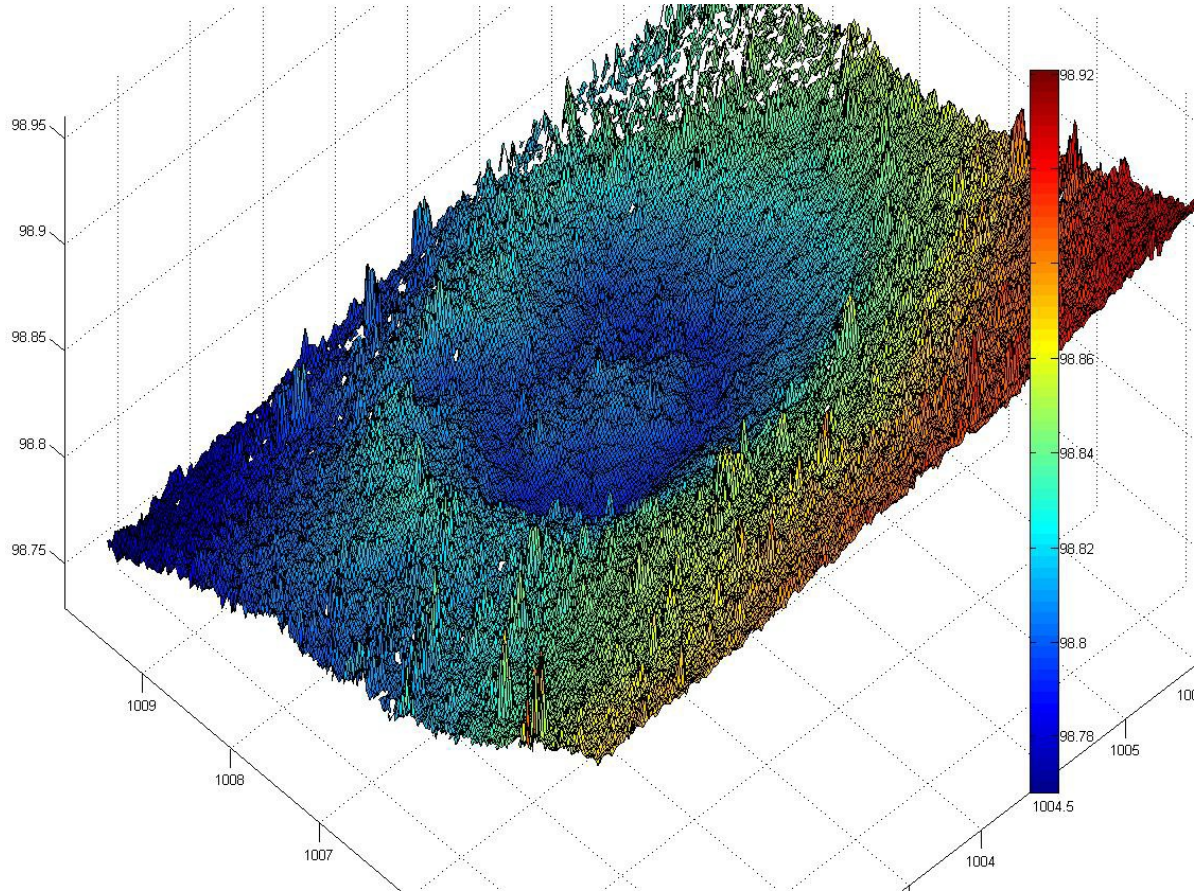

Figure 35. Example of a small, circular depression in a desert pavement surface rendered from LiDAR data using MATLAB. Vertical relief (m) is expressed with the stretched color scale (right); horizontal and vertical axes have units in meters. Two cm-scale means that z(x, y) is median of all z-values in the 2 cm cell. Notice that the center is not the lowest point of the interior; there is a low ring around the center. This particular feature of the depression is not readily apparent without a high-resolution surface image of the kind produced during LiDAR scanning. This image shows a TIN surface of the raw, unprocessed LiDAR dataset for this feature; smoothing algorithms and dataset cleaning to remove point reflections by vegetation (anomalous, isolated peaks) will produce clearer graphical outputs.

Methods for effectively evaluating microtopography and surface roughness are currently under review. In recent research, surface roughness has been quantified for alluvial landforms of varying age from airborne LiDAR. Using this quantification as a predictive tool, researchers have shown that distinct roughness signatures have proven effective as a means for distinguishing between landforms, at least at the macrotopographic scale. It is currently unknown whether this roughness distinction is pervasive at the microtopographic scale, but the datasets from the Yuma Proving Ground scans will play an important role in this determination. At present, we continue to optimize our ability to visualize these datasets using readily-available tools, and will continue to refine analytical methods to quantify surface roughness.

3. Detailed Terrain Analysis Studies

3.1.2 Characterization of the terrain and surface soil conditions of vehicle test courses

As part of the GMOE project, and in collaboration with USMA (U.S. Military Academy) and ATEC (U.S. Army Test and Evaluation Command), comprehensive surface soil and landform characterization has been carried out for vehicle test courses at six US Army installations, including Yuma Proving Ground, Aberdeen Proving Ground, Fort AP Hill, Alaska Ft. Greely, Panama, and Suriname. Together these locations span a broad range of climatic and physiographic settings, which means that in addition to the site specific utility of the datasets, they comprise information on analogs for a range of biomes including desert (YPG), tropical (Suriname and Panama), cold (Alaska), and temperate (AP Hill and APG) regimes. Therefore, these datasets will help in assessing trafficability and vehicle testing requirements in a range of possible deployment locations.

Data collected includes geotechnical engineering data, soil characterization data (both geological and engineering classification systems), landform classifications, and in some cases, iPix panoramic photographs. Data collection took place at pre-determined sites at set distances along each course. Samples for soil characterization were taken from two depths – 0-6 inches, and 6-12 inches – and analyzed at the DRI Soil Characterization and Quaternary Pedology Lab. The focus was on particle size analysis, which was carried out using a combination of sieving and laser diffraction analysis, but select samples were also measured for soluble salt content, carbonate content, and Fe oxide content. Geotechnical data collected includes Stiffness and Young's Modulus (measured by a Geogauge); and bulk density and water content (measured by a nuclear density gauge). At some installations, geotechnical data and sample collection was carried out by U.S. Army Cadets; landform classifications, however, were carried out by trained geomorphologists through field and map observations.

Potential innovative applications of this data include the development of interactive geodatabases to provide a user friendly map-based product that allows test engineers and army personnel to quickly access and visualize pertinent data for each test course. To illustrate this type of application, Figures 36 and 37 show an interactive map-based database that was created for the Suriname test course. All data was compiled and presented in a GIS platform. Figure 36 is a summary sheet of all data obtained for a particular site along the course, showing how it compares to other locations; and Figure 37 shows a screen shot of the final product: a map of the course may be viewed and data for any particular site pulled up with one click of the mouse. Data for the other test courses included in this effort are currently represented in tabular, and (in the case of grain size/grading), graphical form; but are available for future integration into such comprehensive map-based products.

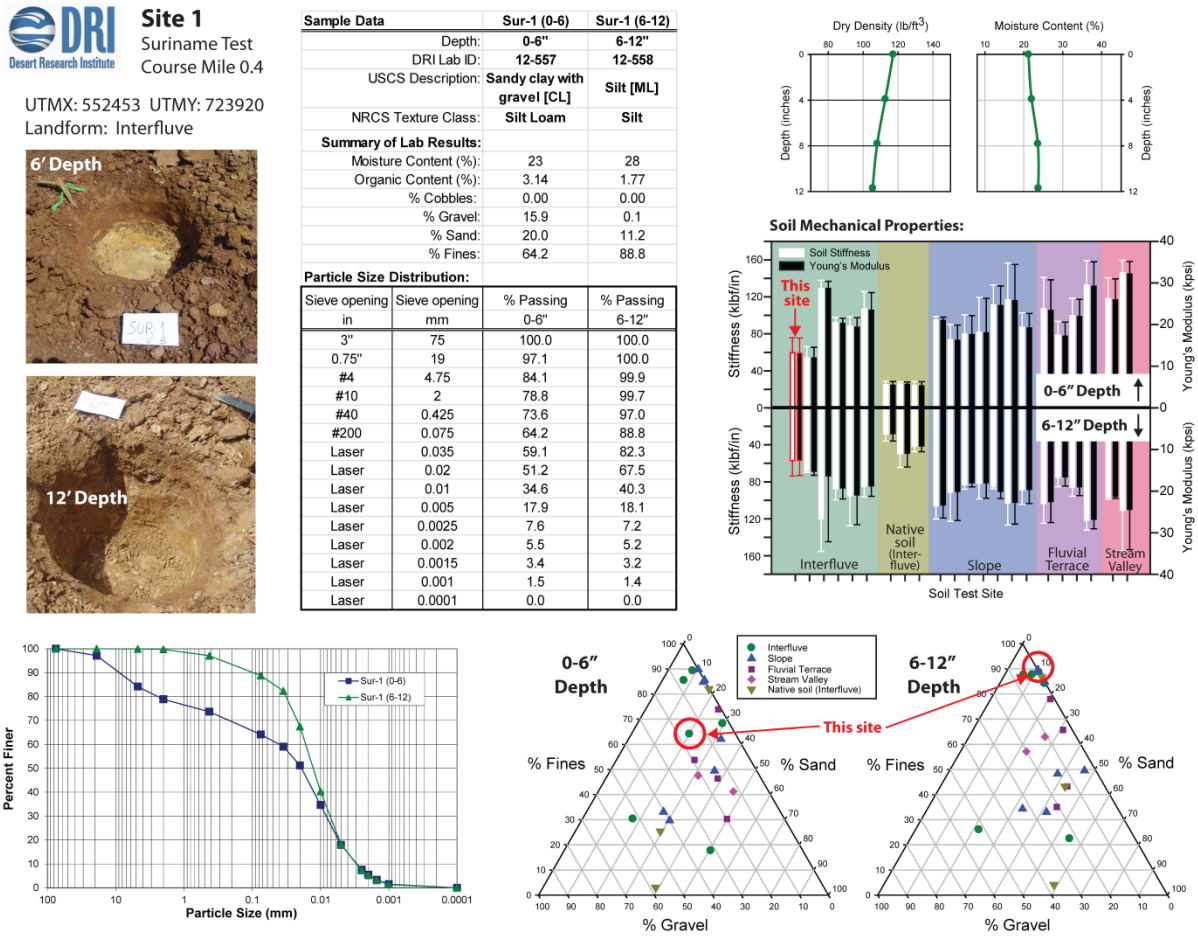

Figure 36. Example of a datasheet that can be produced for each individual sampling site along the vehicle test courses characterized. This sheet is for Site 1 of the Suriname Test Course.

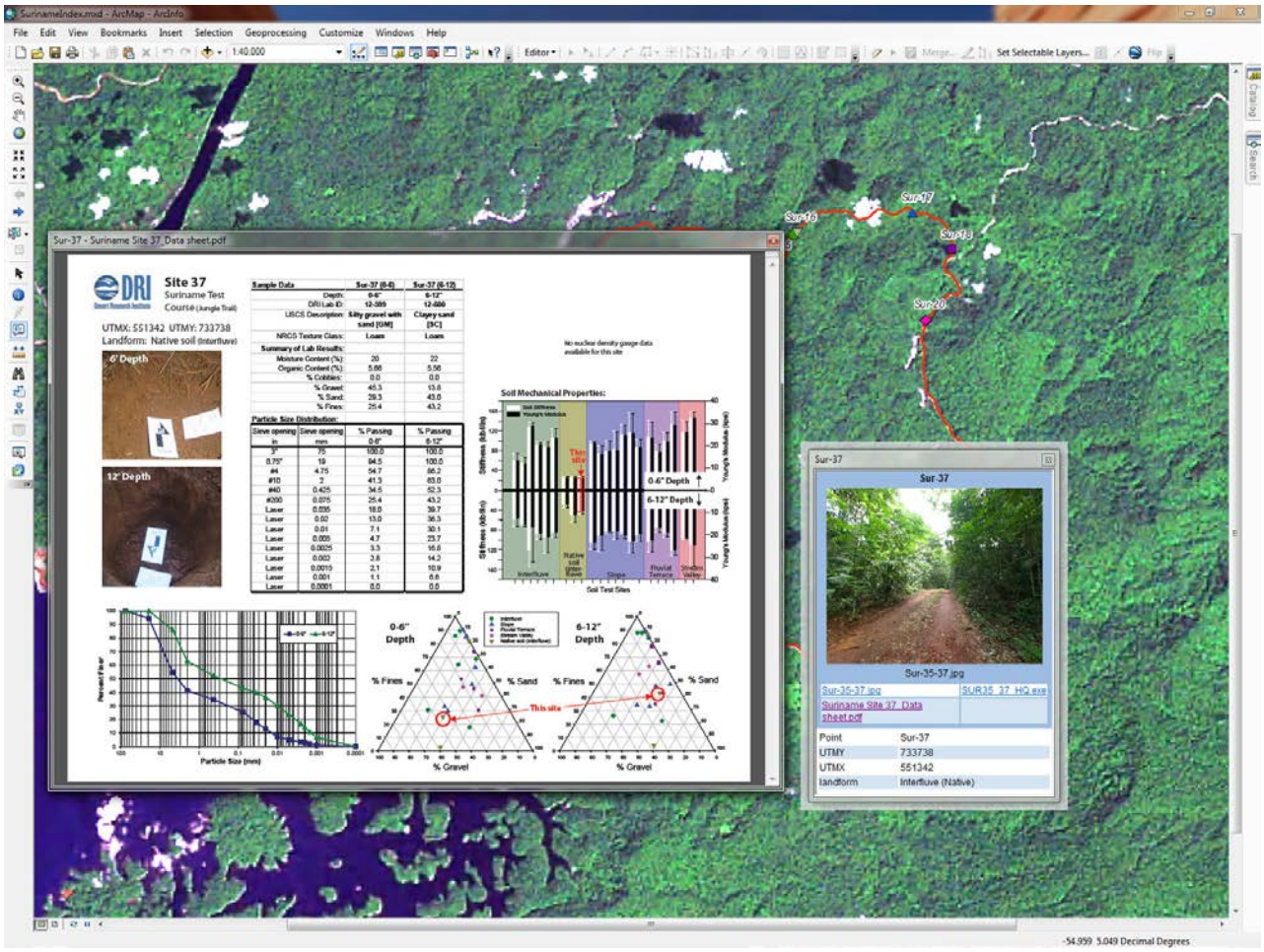

Figure 37. Screen shot of the interactive map-based database that was created for the Suriname vehicle test course.

4. Manuscripts and theses directly resulting from this project

Bacon, S.N., McDonald, E.V., Amit, R., Enzel, Y., and Crouvi, O., 2011, Total suspended particulate matter emissions at high friction velocities from desert landforms: Journal of Geophysical Research, v. 116, p. F03.

Caldwell, T.G., 2011, Soil Heterogeneity in Arid Shrublands: Biotic and Abiotic Processes: PhD thesis, University of Reno.

Caldwell, T.G., McDonald, E., Mihevc, T.M., Bacon, S., Baker, S., and Susfalk, R.B., In preparation, Monitoring the electrical and thermal properties of disturbed soils for military operations. 9th International Conference on Military Geosciences – Conference Proceedings. June 20-24, 2011, Las Vegas, NV.

Caldwell, T.G., Wohling, T., Young, M.H., Boyle, D.P., and McDonald, E., 2012, Characterizing disturbed desert soils using multiobjective inverse parameter optimization: Vadose Zone Journal, v. In revision.

Caldwell, T.G., Young, M.H., McDonald, E.V., and Zhu, J.T., 2012, Soil heterogeneity in Mojave Desert shrublands: Biotic and abiotic processes: Water Resources Research, v. 48.

Flerchinger, G.N., Caldwell, T.G., Cho, J., and Hardegree, S.P., 2012, Simultaneous Heat and Water (SHAW) Model: Model use, calibration, and validation: Transactions of the ASABE, v. 55, p. 1395-1411.

Regmi, N.R., McDonald, E., and Bacon, S., 2013, Mapping Quaternary Alluvial Fans in the Southwestern United States based on Multi-Parameter Surface Roughness of LiDAR Topographic Data: Journal of Geophysical Research - Earth Surface, v. Submitted.

5. Manuscripts resulting from related and collaborative work

Bacon, S.N., McDonald, E.V., Baker, S.E., Caldwell, T.G., and Stullenbarger, G., 2008, Desert terrain characterization of landforms and surface materials within vehicle test courses at U.S. Army Yuma Proving Ground, USA: Journal of Terramechanics, v. 45, p. 167-183.

Caldwell, T.G., McDonald, E.V., Bacon, S.N., and Stullenbarger, G., 2008, The performance and sustainability of vehicle dust courses for desert military testing: Journal of Terramechanics, v. 45, p. 213-221.

Crouvi, O., Rivka, A., Porat, N., Gillespie, A.R., McDonald, E.V., and Enzel, Y., 2009, Significance of primary hilltop loess in reconstructing dust chronology, accretion rates, and sources; an example from the Negev Desert, Israel: Journal of Geophysical Research, v. 114.